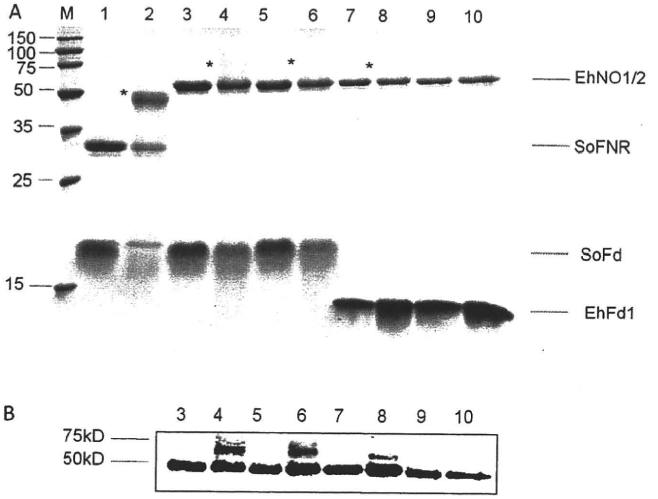

FIGURE 4. ***In vitro* interactions of EhNO with ferredoxin.** *A*, SDS-PAGE analysis of the complex of EhNO and ferredoxin is shown. Protein mixtures were incubated for 30 min with (*even lane numbers*) and without (*odd lane numbers*) 5 mM carbodiimide, electrophoresed on a 15% SDS-PAGE gel under reducing conditions, and then stained with Coomassie Brilliant Blue R250. The examined protein mixtures were as follows: *lanes 1* and *2*, spinach (*S. oleracea*) ferredoxin:NADP$^+$ reductase (*SoFNR*) + spinach ferredoxin (*SoFd*); *lanes 3* and *4*, *EhNO1+SoFd*; *lanes 5* and *6*, *EhNO2+SoFd*; *lanes 7* and *8*, *EhNO1+EhFd1*; *lanes 9* and *10*, *EhNO2+EhFd1*. Protein bands corresponding to the cross-linked proteins are indicated by an *asterisk*. The positions of the purified proteins are indicated on the *right side of the gel*. *B*, shown is an immunoblot analysis of the cross-linked samples using an anti-His antibody.

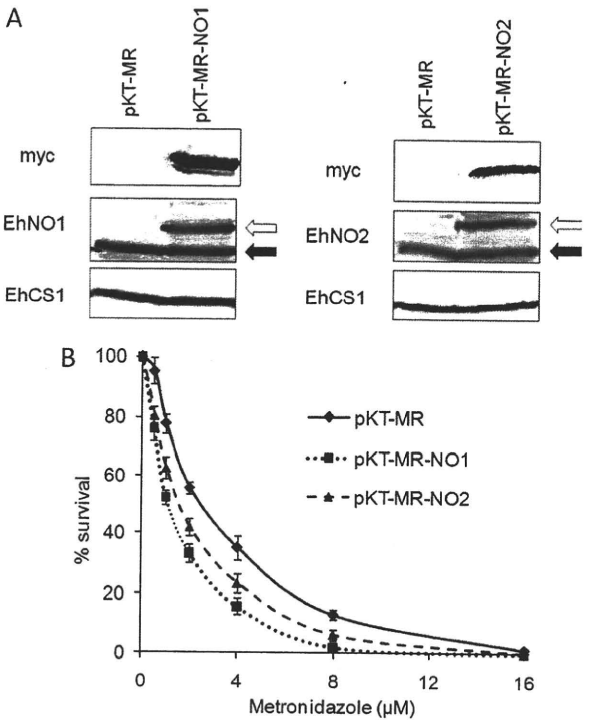

FIGURE 5. **Changes in the sensitivity of *E. histolytica* to metronidazole by overexpression of EhNOs.** *A*, shown is an immunoblot analysis of EhNOs in the transformants expressing Myc-tagged EhNO1 and -2. Approximately 40 μg of total lysate from the pKT-MR (control), EhNO1 (*pKT-MR-NO1*), and EhNO2 (*pKT-MR-NO2*)-overexpressing transformants was electrophoresed on a SDS-PAGE gel under reducing conditions and subjected to immunoblot analysis using anti-EhNO1, anti-EhNO2, anti-Myc, and anti-EhCS1 (*control*) antibodies. *Black* and *white arrows* indicate endogenous and Myc-tagged EhNO1 and -2, respectively. *B*, susceptibility of transformed trophozoites to metronidazole is shown. Trophozoites (10^4 cells/ml) were cultivated in the presence of 0–16 μM metronidazole for 48 h, and the number of viable cells was then counted. The percentages of living cells are shown relative to those of unexposed control cells. *Error bars* represent the S.E. of five independent experiments.

physically interacted with homologous and heterologous (*Spinacia oleracea*) ferredoxin (SoFd) using a carbodiimide-promoted cross-linking (50). We first cloned and purified a representative [3Fe4S] ferredoxin found in the *E. histolytica* genome data base (EhFd1; TIGR ID 128.m00136). For the assay, rEhNO1 and -2 were mixed with either purified EhFd1 or SoFd, cross-linked, and then analyzed by SDS-PAGE (Fig. 4*A*). It was observed that both rEhNO1 and -2 formed a complex with spinach ferredoxin, as shown by the appearance of a large 60-kDa band in the gel and more easily observed in the Western blot analysis using an anti-histidine antibody (Fig. 4*B*, *lanes 4* and *6*). However, only EhNO1 formed a complex with *E. histolytica* ferredoxin (EhFd1) (Fig. 4, *A* and *B*, *lanes 8* and *10*).

Cellular Distribution of EhNO—We also examined the cellular distribution of EhNO1 and -2 in trophozoites. The immunofluorescence imaging using antiserum raised against the corresponding recombinant protein revealed that the two isotypes were distributed throughout the cytosol (data not shown). We also verified the localization of EhNOs by immunoblotting using lysates produced by a Dounce glass homogenizer followed by sonication and centrifugation at 100,000 × *g* at 4 °C for 1 h. Both EhNO1 and -2 fractionated into the soluble fraction (data not shown).

Increased Metronidazole Sensitivity by EhNO Overexpression—To confirm that EhNO is the target of metronidazole in *E. histolytica*, stable transformants that overexpressed Myc-tagged EhNO1 or 2 were generated. Both the transformants expressing Myc-tagged EhNO1 or EhNO2 expressed ~2-fold higher levels of the corresponding enzymes than the control (Fig. 5*A*) and were more sensitive to metronidazole. The 50% growth inhibitory concentrations (IC_{50}) of metronidazole for the Myc-EhNO1- and Myc-EhNO2-overexpressing transformants were 1.03 ± 0.05 and 1.42 ± 0.12 μM, respectively (Fig. 5*B*), whereas the control showed an IC_{50} of 2.24 ± 0.33 μM.

DISCUSSION

In the present study we demonstrated novel enzymatic reactions catalyzed by a new class of FAD- and 2[4Fe-4S]-containing NADPH-dependent oxidoreductases from *E. histolytica*, which had been initially discovered by virtue of tightly regulated gene expression in correlation with L-cysteine concentrations. Although the two EhNOs characterized in this study had been annotated before this study based on their high degree of homology with GOGAT β subunit and β subunit-like genes from a variety of organisms, their biochemical function was unknown. The fact that the two EhNOs shared significant similarity with homologs from archaeal organisms raised the question of whether they represented a prototype GOGAT protein, similar to the β subunit protein from *Pyrococcus*, which was reported to possess NADPH-dependent GOGAT activity and be capable of both glutamine and ammonia-dependent synthesis in the absence of the α subunit (7). However, we were unable to observe glutamate synthase activity of the EhNOs under similar conditions used for the *Pyrococcus* glutamate synthase. Fur-

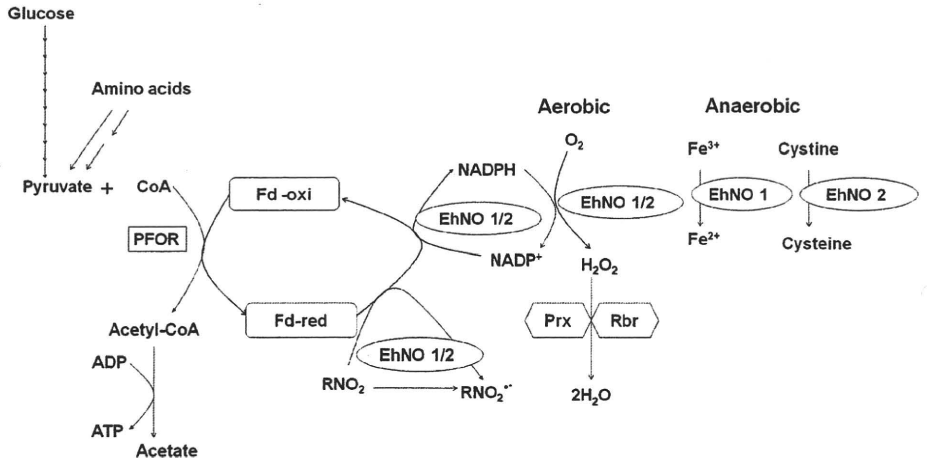

FIGURE 6. **Proposed *in vivo* reactions catalyzed by EhNO1 and -2.** *PFOR*, pyruvate:ferredoxin oxidoreductase; *Fd-red* and *Fd-oxi*, reduced and oxidized form of ferredoxin; *Prx*, peroxiredoxin; *Rbr*, rubrerythrin; RNO_2/$RNO_2^{\bullet-}$, metronidazole/reduced metronidazole.

thermore, the expression of the GOGAT β subunit failed to restore glutamate auxotrophy in an *E. coli* GOGAT α subunit-deficient strain (5, 51). In addition, it was somewhat puzzling how the *Pyrococcus* GOGAT β subunit functioned in substrate binding and catalysis without the α subunit, which has been shown to be responsible for substrate recognition (52). Thus, it was thought that the EhNO β subunit-like proteins may be involved in reactions other than glutamate synthesis.

The physiological roles of EhNO1 and EhNO2 have not been unequivocally demonstrated because our attempt to repress EhNO expression by gene silencing (53) failed (data not shown), and gene knock-out has not been accomplished in *E. histolytica*. Nevertheless, our present enzymological characterization revealed the physiological significance of the presence of the two isotypes of EhNOs. EhNO2 appears to play an important role in the reduction of cystine to L-cysteine. Because L-cysteine is partially present in the oxidized form inside cells (CE-MS analysis, Fig. 2*B*), L-cystine reduction is necessary before the utilization of L-cysteine, which has been implicated in the attachment to matrix, elongation, motility, growth, and anti-oxidative defense (35, 54, 55). Transcriptomic analysis demonstrated that the transcription of EhNO2, but not EhNO1, is tightly regulated by extracellular L-cysteine concentrations. Furthermore, the measured kinetic parameters indicate that EhNO2 possesses 4-fold higher L-cystine reduction efficiency than EhNO1.

The acquisition of iron and subsequent assimilation into cellular proteins are ubiquitously essential for life. However, at physiological pH under aerobic conditions, iron is present as Fe^{3+} hydroxides and oxyhydroxides or in a complex with ferric-specific chelators, *e.g.* siderophores (56). Subsequent reduction of complexed Fe^{3+} is accomplished by ferric reductases using NAD(P)H as the electron donor (57), with the resulting Fe^{2+} being subsequently released and incorporated into iron-containing proteins (58). We showed that rEhNO1 catalyzes the reduction of ferric ion >100-fold more efficiently than rEhNO2 (Table 2), suggesting that EhNO1 is mainly involved in ferric reduction. We also confirmed that EhNO1 functions as a ferredoxin:$NADP^+$ reductase, similar to the recently reported ferric reductase from *Pseudomonas putida* (59), by catalyzing reversible electron transfer between one molecule of $NADP^+$/NADPH and two molecules of ferredoxin. *In vitro* cross-linking of the two EhNOs with ferredoxin indicate that only EhNO1 forms a stable complex with *E. histolytica* ferredoxin (EhFd1), whereas both EhNO1 and EhNO2 physically interact with spinach ferredoxin (Fig. 4*B*), indicating that the specificity toward ferredoxin differs between these two proteins. The *E. histolytica* genome encodes four types of ferredoxins which are highly divergent at the primary sequence level and also in the Fe-S clusters. We, therefore, hypothesize that EhNO2 interacts with a ferredoxin(s) other than EhFd1 in *E. histolytica*, a speculation that is supported by the observed differential binding of photosynthetic and non-photosynthetic maize ferredoxins to root *Zea mays* ferredoxin:$NADP^+$ reductase (60).

E. histolytica is anaerobic/microaerophilic and possesses highly degenerated mitochondria that are incapable of oxidative phosphorylation and ATP generation. A crucial step in energy production via glycolysis and fermentation in *E. histolytica* involves the decarboxylation of pyruvate to acetyl CoA that is catalyzed by pyruvate:ferredoxin oxidoreductase (61). Concomitant with the decarboxylation of pyruvate, an electron is transferred to oxidized ferredoxin. Generally, reduced ferredoxin subsequently donates an electron to NAD(P) by the action of ferredoxin:NADP reductase, which serves to regenerate the intracellular pools of NAD(P)H and oxidized ferredoxin. However, as the *Entamoeba* genome does not contain an ferredoxin:NADP reductase homolog, it was unclear how NAD(P)H was regenerated. Our enzymological study indicates that EhNOs, and EhNO1 in particular, function as ferredoxin:NADP reductases and are involved in the regeneration of NADPH and oxidized ferredoxin required for continuous energy production.

As stated above, *E. histolytica* possesses highly divergent mitochondria (62) and lacks a functional tricarboxylic acid cycle, cytochromes, and a conventional respiratory electron transport chain terminating in the reduction of oxygen to water. However, amebae can still tolerate up to 5% of oxygen in the gas phase (63, 64) and consume oxygen (65). As shown here, EhNOs are flavoproteins containing 1 mol of FAD as a prosthetic group per mol of enzyme. During the NADPH:flavin oxidoreductase reaction, NADPH binds to EhNOs, and two electrons are transferred to FAD to yield $FADH_2$, which is immediately dissociated from the enzyme (66). Under aerobic conditions, $FADH_2$ is rapidly oxidized by molecular oxygen to yield H_2O_2 and FAD (67). As *E. histolytica* amebae do not produce detectable amounts of H_2O_2 (27), it is possible that H_2O_2 is further converted to water by peroxiredoxin (68) and rubrerythrin (69) to overcome oxidative stress. Under anaero-

bic conditions, EhNO1 catalyzes ferric ion reduction, whereas EhNO2 catalyzes cystine reduction. Based on the demonstrated reactions catalyzed by the two EhNOs, we have proposed functional roles for these two proteins in *E. histolytica* that are summarized in Fig. 6.

Metronidazole is a prodrug currently used to treat a number of microbial infections, and its activation requires intracellular reduction to produce cytotoxic short-lived radicals and other reactive species (70). *Entamoeba* electron transport proteins, which have been reported to provide the source of electrons for the reductive activation of metronidazole, include ferredoxin (71), thioredoxin reductase (72), and nitroreductase (49). We demonstrated that both EhNO1 and -2 catalyze metronidazole reduction *in vitro* (Table 1), and their overexpression confers increased sensitivity to this drug (Fig. 5*B*). This finding suggests that in addition to ferredoxin (71), pyruvate:ferredoxin oxidoreductase (71), thioredoxin (72), and nitroreductase (49), EhNO1 and -2 are also involved in metronidazole activation in *E. histolytica*.

In conclusion, we have demonstrated for the first time that two novel NADPH-dependent GOGAT small subunit-like proteins of *E. histolytica* function, at least *in vitro*, as cystine/ferric/ferredoxin:$NADP^+$ reductase. We propose that they play a role in maintaining intracellular redox potential and may be responsible for metronidazole activation in this parasite. The physiological substrates and biological roles of the majority of oxidoreductases discovered by genome mining remain largely unknown. Vigorous attempts to discover the substrates and functions of individual oxidoreductases should unveil novel cellular metabolic processes in pathogens and cancer cells that may lead to the development of new chemotherapeutics.

Acknowledgments—We thank Kumiko Nakada-Tsukui, Fumika Michi, Takashi Makiuchi, and all other members of our laboratory for technical assistance and valuable discussions.

REFERENCES

1. Ratti, S., Curti, B., Zanetti, G., and Galli, E. (1985) *J. Bacteriol.* **163,** 724–729
2. Rosenbaum, K., Jahnke, K., Curti, B., Hagen, W. R., Schnackerz, K. D., and Vanoni, M. A. (1998) *Biochemistry* **37,** 17598–17609
3. Tóth, A., Takács, M., Groma, G., Rákhely, G., and Kovács, K. L. (2008) *FEMS Microbiol. Lett.* **282,** 8–14
4. Vanoni, M. A., and Curti, B. (1999) *Cell Mol. Life Sci.* **55,** 617–638
5. Stutz, H. E., and Reid, S. J. (2004) *Biochim. Biophys. Acta* **1676,** 71–82
6. Saum, S. H., Sydow, J. F., Palm, P., Pfeiffer, F., Oesterhelt, D., and Müller, V. (2006) *J. Bacteriol.* **188,** 6808–6815
7. Jongsareejit, B., Rahman, R. N., Fujiwara, S., and Imanaka, T. (1997) *Mol. Gen. Genet.* **254,** 635–642
8. World Health Organization (1997) *WHO/PAHO/UNESCO Report: A consultation with experts on amebiasis. Mexico City, Mexico 28–29 January, 1997. Epidemiol. Bull* **18,** 13–14
9. Upcroft, P., and Upcroft, J. A. (2001) *Clin. Microbiol. Rev.* **14,** 150–164
10. Hoffman, J. S., and Cave, D. R. (2001) *Curr. Opin. Gastroenterol.* **17,** 30–34
11. World Health Organization (2007 March) *WHO Model List of Essential Medicines,* 15th Ed.
12. Müller, M. (1983) *Surgery* **93,** 165–171
13. Moreno, S. N., and Docampo, R. (1985) *Environ. Health Perspect.* **64,** 199–208
14. West, S. B., Wislocki, P. G., Fiorentini, K. M., Alvaro, R., Wolf, F. J., and Lu,, A. Y. (1982) *Chem. Biol. Interact.* **41,** 265–279
15. Ludlum, D. B., Colinas, R. J., Kirk, M. C., and Mehta, J. R. (1988) *Carcinogenesis* **9,** 593–596
16. Diamond, L. S., Harlow, D. R., and Cunnick, C. C. (1978) *Trans. R. Soc. Trop. Med. Hyg.* **72,** 431–432
17. Clark, C. G., and Diamond, L. S. (2002) *Clin. Microbiol. Rev.* **15,** 329–341
18. Thompson, J. D., Higgins, D. G., and Gibson, T. J. (1994) *Nucleic Acids Res.* **22,** 4673–4680
19. Leão-Helder, A. N., Krikken, A. M., Gellissen, G., van der Klei, I. J., Veenhuis, M., and Kiel, J. A. (2004) *FEBS Lett.* **577,** 491–495
20. Kumar, S., Tamura, K., Jakobsen, I. B., and Nei, M. (2001) *Bioinformatics* **17,** 1244–1245
21. Sambrook, J., and Russell, D. W. (2001) *Molecular Cloning: A Laboratory Manual,* 3rd Ed., Cold Spring Harbor Laboratory Press, Cold Spring Harbor, NY
22. Nozaki, T., Asai, T., Kobayashi, S., Ikegami, F., Noji, M., Saito, K., and Takeuchi, T.. (1998) *Mol. Biochem. Parasitol.* **97,** 33–44
23. Bradford, M. M. (1976) *Anal. Biochem.* **72,** 248–254
24. Faeder, E. J., and Siegel, L. M. (1973) *Anal. Biochem.* **53,** 332–336
25. Olson, J. W., Agar, J. N., Johnson, M. K., and Maier, R. J. (2000) *Biochemistry* **39,** 16213–16219
26. Chen, J. S., and Blanchard, D. K. (1979) *Anal. Biochem.* **93,** 216–222
27. Lo, H., and Reeves, R. E. (1980) *Mol. Biochem. Parasitol.* **2,** 23–30
28. Ichikawa, Y., Hiwatashi, A., Yamano, T., Kim, H. J., and Maruya, N. (1980) in *Flavins and Flavoproteins* (Yagi, K., and Yamano, T., eds) pp. 677–691, University Park Press, Baltimore, MD
29. Thurman, R. G., Ley, H. G., and Scholz, R. (1972) *Eur. J. Biochem.* **25,** 420–430
30. Soga, T., and Heiger, D. N. (2000) *Anal. Chem.* **72,** 1236–1241
31. Soga, T., Ohashi, Y., Ueno, Y., Naraoka, H., Tomita, M., and Nishioka, T. (2003) *J. Proteome Res.* **2,** 488–494
32. Soga, T., Baran, R., Suematsu, M., Ueno, Y., Ikeda, S., Sakurakawa, T., Kakazu, Y., Ishikawa, T., Robert, M., Nishioka, T., and Tomita, M. (2006) *J. Biol. Chem.* **281,** 16768–16776
33. Ohashi, Y., Hirayama, A., Ishikawa, T., Nakamura, S., Shimizu, K., Ueno, Y., Tomita, M., and Soga, T. (2008) *Mol. Biosyst.* **4,** 135–147
34. Nakada-Tsukui, K., Okada, H., Mitra, B. N., and Nozaki, T. (2009) *Cell. Microbiol.* **11,** 1471–1491
35. Nozaki, T., Asai, T., Sanchez, L. B., Kobayashi, S., Nakazawa, M., and Takeuchi, T. (1999) *J. Biol. Chem.* **274,** 32445–32452
36. Zanetti, G., Morelli, D., Ronchi, S., Negri, A., Aliverti, A., and Curti, B. (1988) *Biochemistry* **27,** 3753–3759
37. Tokoro, M., Asai, T., Kobayashi, S., Takeuchi, T., and Nozaki, T. (2003) *J. Biol. Chem.* **278,** 42717–42727
38. Nakada-Tsukui, K., Saito-Nakano, Y., Ali, V., and Nozaki, T. (2005) *Mol. Biol. Cell* **16,** 5294–5303
39. Srivastava, M., Ahmad, N., Gupta, S., and Mukhtar, H. (2001) *J. Biol. Chem.* **276,** 15481–15488
40. Loftus, B., Anderson, I., Davies, R., Alsmark, U. C., Samuelson, J., Amedeo, P., Roncaglia, P., Berriman, M., Hirt, R. P., Mann, B. J., Nozaki, T., Suh, B., Pop., M., Duchene, M., Ackers, J., Tannich, E., Leippe, M., Hofer, M., Bruchhaus, I., Willhoeft, U., Bhattacharya, A., Chillingworth, T., Churcher, C., Hance, Z., Harris, B., Harris, D., Jagels, K., Moule, S., Mungall, K., Ormond, D., Squares, R., Whitehead, S., Quail, M. A., Rabbinowitsch, E., Norbertczak, H., Price, C., Wang, Z., Guillén, N., Gilchrist, C., Stroup, S. E., Bhattacharya, S., Lohia, A., Foster, P. G., Sicheritz-Ponten, T., Weber, C., Singh, U., Mukherjee, C., El-Sayed, N. M., Petri, W. A., Jr, Clark, C. G., Embley, T. M., Barrell, B., Fraser, C. M., and Hall, N. (2005) *Nature* **433,** 865–868
41. Morandi, P., Valzasina, B., Colombo, C., Curti, B., and Vanoni, M. A. (2000) *Biochemistry* **39,** 727–735
42. Pelanda, R., Vanoni, M. A., Perego, M., Piubelli, L., Galizzi, A., Curti, B., and Zanetti, G. (1993) *J. Biol. Chem.* **268,** 3099–3106
43. Andersson, J. O., and Roger, A. J. (2002) *Eukaryot. Cell* **1,** 304–310
44. Gillin, F. D., and Diamond, L. S. (1981) *Exp. Parasitol.* **51,** 382–391
45. Latimer, M. T., Painter, M. H., and Ferry, J. G. (1996) *J. Biol. Chem.* **271,** 24023–24028
46. Fontecave, M., Eliasson, R., and Reichard, P. (1987) *J. Biol. Chem.* **262,** 12325–12331

47. Jablonski, E., and DeLuca, M. (1978) *Biochemistry* **17,** 672–678
48. Foust, G. P., Mayhew, S. G., and Massey, V. (1969) *J. Biol. Chem.* **244,** 964–970
49. Pal, D., Banerjee, S., Cui, J., Schwartz, A., Ghosh, S. K., and Samuelson, J. (2009) *Antimicrob. Agents Chemother.* **53,** 458–464
50. Zanetti, G., Aliverti, A., and Curti, B. (1984) *J. Biol. Chem.* **259,** 6153–6157
51. Deane, S. M., and Rawlings, D. E. (1996) *Gene* **177,** 261–263
52. Vanoni, M. A., Fischer, F., Ravasio, S., Verzotti, E., Edmondson, D. E., Hagen, W. R., Zanetti, G., and Curti, B. (1998) *Biochemistry* **37,** 1828–1838
53. Bracha, R., Nuchamowitz, Y., Anbar, M., and Mirelman, D. (2006) *PLoS Pathog.* **2,** e48
54. Gillin, F. D., and Diamond, L. S. (1981) *Exp. Parasitol.* **52,** 9–17
55. Gillin, F. D., and Diamond, L. S. (1980) *J. Protozool.* **27,** 474–478
56. Barchini, E., and Cowart, R. E. (1996) *Arch. Microbiol.* **166,** 51–57
57. Lesuisse, E., Crichton, R. R., and Labbe, P. (1990) *Biochim. Biophys. Acta* **1038,** 253–259
58. Guerinot, M. L. (1994) *Annu. Rev. Microbiol.* **48,** 743–772
59. Yeom, J., Jeon, C. O., Madsen, E. L., and Park, W. (2009) *J. Bacteriol.* **191,** 1472–1479
60. Onda, Y., Matsumura, T., Kimata-Ariga, Y., Sakakibara, H., Sugiyama, T., and Hase, T. (2000) *Plant Physiol.* **123,** 1037–1045
61. Kerscher, L., and Oesterhelt, D. (1982) *Trends Biol. Sci.* **7,** 371–374
62. Tovar, J., Fischer, A., and Clark, C. G. (1999) *Mol. Microbiol.* **32,** 1013–1021
63. Band, R. N., and Cirrito, H. (1979) *J. Protozool.* **26,** 282–286
64. Reeves, R. E. (1984) *Adv. Parasitol.* **23,** 105–142
65. Weinbach, E. C., and Diamond, L. S. (1974) *Exp. Parasitol.* **35,** 232–243
66. Inouye, S. (1994) *FEBS Lett.* **347,** 163–168
67. Gibson, Q. H., and Hastings, J. W. (1962) *Biochem. J.* **83,** 368–377
68. Bruchhaus, I., Richter, S., and Tannich, E. (1997) *Biochem. J.* **326,** 785–789
69. Maralikova, B., Ali, V., Nakada-Tsukui, K., Nozaki, T., van der Giezen, M., Henze, K., and Tovar, J. (2010) *Cell Microbiol.* **12,** 331–342
70. Goldman, P., Koch, R. L., Yeung, T. C., Chrystal, E. J., Beaulieu, B. B., Jr., McLafferty, M. A., and Sudlow, G. (1986) *Biochem. Pharmacol.* **35,** 43–51
71. Müller, M. (1986) *Biochem. Pharmacol.* **35,** 37–41
72. Leitsch, D., Kolarich, D., Wilson, I. B. H., Altmann, F., and Duchene, M. (2007) *PLoS Biol.* **5,** e211

Experimental Parasitology 126 (2010) 337–347

Contents lists available at ScienceDirect

Experimental Parasitology

journal homepage: www.elsevier.com/locate/yexpr

Minireview

Conservation and function of Rab small GTPases in *Entamoeba*: Annotation of *E. invadens* Rab and its use for the understanding of *Entamoeba* biology

Kumiko Nakada-Tsukui, Yumiko Saito-Nakano, Afzal Husain, Tomoyoshi Nozaki *

Department of Parasitology, National Institute of Infectious Diseases, Tokyo 162-8640, Japan

ARTICLE INFO

Article history:
Received 7 November 2009
Received in revised form 19 April 2010
Accepted 19 April 2010
Available online 29 April 2010

Keywords:
Entamoeba
Rab
Small GTPase
Vesicular traffic
Encystation

ABSTRACT

Entamoeba invadens is a reptilian enteric protozoan parasite closely related to the human pathogen *Entamoeba histolytica* and a good model organism of encystation. To understand the molecular mechanism of vesicular trafficking involved in the encystation of *Entamoeba*, we examined the conservation of Rab small GTPases between the two species. *E. invadens* has over 100 Rab genes, similar to *E. histolytica*. Most of the Rab subfamilies are conserved between the two species, while a number of species-specific Rabs are also present. We annotated all *E. invadens* Rabs according to the previous nomenclature [Saito-Nakano, Y., Loftus, B.J., Hall, N., Nozaki, T., 2005. The diversity of Rab GTPases in *Entamoeba histolytica*. Experimental Parasitology 110, 244–252]. Comparative genomic analysis suggested that the fundamental vesicular traffic machinery is well conserved, while there are species-specific protein transport mechanisms. We also reviewed the function of Rabs in *Entamoeba*, and proposed the use of the annotation of *E. invadens* Rab genes to understand the ubiquitous importance of Rab-mediated membrane trafficking during important biological processes including differentiation in *Entamoeba*.

1. Introduction

Small GTP-binding proteins (GTPase) are molecular switches ubiquitously found in eukaryotes. These proteins are involved in various important cellular processes including cell proliferation, cytoskeletal assembly, and intracellular membrane traffic. Small GTPases are classified, based on their primary sequences, into five families: Ras, Rho/Rac, Rab, Sar/Arf, and Ran (Bourne et al., 1990; Takai et al., 2001). Rab small GTPases constitute the largest group of this superfamily and are essential regulators of vesicular transport (Novick and Zerial, 1997; Stenmark, 2009). Higher eukaryotes generally have a larger repertoire of Rab genes than unicellular eukaryotes. *Homo sapiens*, *Arabidopsis thaliana*, and *Drosophila melanogaster*, for example, have 60, 29, and 29 Rab genes, respectively, while *Saccharomyces cerevisiae* has only 11 (Pereira-Leal and Seabra, 2001).

Membrane traffic plays an important role in the virulence of the protozoan parasite *Entamoeba histolytica*, the causative agent of amebiasis. Regulation of membrane trafficking via Rab proteins has been well studied in *E. histolytica* (for a review, see Nozaki and Nakada-Tsukui, 2006). While a majority of parasitic protozoa possess reduced numbers of Rab genes, *E. histolytica* and *Trichomonas vaginalis* have an expanded repertoire of Rabs (Saito-Nakano et al., 2005; Carlton et al., 2007), suggesting that they rely heavily on Rab-mediated membrane trafficking. Among the more than 100 Rabs identified to date, the functions of only a half dozen *E. histolytica* Rabs, that is, EhRabA, 5, 7A, 7B, 11A, and 11B, have been demonstrated (Welter et al., 2005; Welter and Temesvari, 2009; Saito-Nakano et al., 2004; Nakada-Tsukui et al., 2005; Saito-Nakano et al., 2007; Mitra et al., 2007). Thus, the role of the complex Rab family in *Entamoba* has only started to be unveiled.

The molecular mechanisms of stage conversion between the trophozoite and cyst stages remain largely unknown in *E. histolytica* (Eichinger, 1997; Singh and Ehrenkaufer, 2009), due to the lack of an *in vitro* encystation system. Thus, encystation has been studied in *Entamoeba invadens*, a closely related reptilian pathogen that also forms quadranucleate cysts (Eichinger, 2001; Wang et al., 2003). Vesicular traffic likely plays an important role in encystation because the trophozoite degrades unnecessary components and synthesizes and transports new molecules necessary for cyst formation (Picazarri et al., 2008; Chatterjee et al., 2009). In this review, we propose the annotation of Rab genes from *E. invadens* to facilitate the understanding of the conservation and species-specific evolution of Rab in *Entamoeba*. We show that fundamental Rab-mediated vesicular trafficking is well conserved in *Entamoeba*. We also summarize and review previous studies that showed transcriptional changes of Rab genes under stress and during stage conversion in *E. histolytica*, and transcriptional differences between *E. histolytica* strains.

* Corresponding author. Address: Department of Parasitology, National Institute of Infectious Diseases, 1-23-1 Toyama, Shinjuku-ku, Tokyo 162-8640, Japan. Fax: +81 3 5285 1219x1173.
E-mail address: nozaki@nih.go.jp (T. Nozaki).

0014-4894/$ - see front matter © 2010 Elsevier Inc. All rights reserved.
doi:10.1016/j.exppara.2010.04.014

Table 1
Rab small GTPases in *E. histolytica* and *E. invadens*.

Rab subfamily	*Entamoeba histolytica*					*Entamoeba invadens*				
	EhRab isotype	Accession number	ID number	Protein length	C-terminal peptides	EiRab isotype	ID number	% Identity to Eh homologue	Protein length	C-terminal peptides
I. Rab conserved in eukaryotes										
Rab1	EhRab1A	XP_651336	EHI_108610	206	CXXX	EiRab1A	EIN_104660	83	207	CXXX
	EhRab1B	XP_649033	EHI_146510	200	XXCC	EiRab1B	EIN_033160	75	208	CXCX
Rab2	EhRab2A	XP_649924	EHI_146320	785	–	EiRab2A	EIN_200080	59	217	–
	EhRab2B	XP_649335	EHI_046390	214	–	EiRab2B	EIN_277910	84	211	–
	EhRab2C	XP_656786	EHI_067850	232	–					
Rab5	EhRab5	XP_655377	EHI_026420	196	XXCC	EiRab5A	EIN_277000	83	194	XXCC
						EiRab5B	EIN_051650	50[b]	188	XCGC
Rab21	EhRab21	XP_651927	EHI_129330	204	XXCC					
Rab7	EhRab7A	XP_649196	EHI_192810	207	XCXC	EiRab7A	EIN_112310	91	205	XXCC
	EhRab7B	XP_656820	EHI_081330	208	XCXC	EiRab7B	EIN_202680	88	206	XXCC
	EhRab7C	XP_652334	EHI_189990	198	XXCC	EiRab7C	EIN_094230	67	213	XXCC
	EhRab7D	XP_651915	EHI_082070	205	XXCC	EiRab7D	EIN_133760	80	200	XXCC
	EhRab7E	XP_651202	EHI_169280	208	XXCC	EiRab7E	EIN_148860	87	206	XXCC
	EhRab7F	XP_650338	EHI_192130	202	XXCC	EiRab7F	EIN_235870	64	206	XXCC
	EhRab7G	XP_656477	EHI_187090	191	XXCC	EiRab7G1	EIN_015310	62	197	XXCC
						EiRab7G2	EIN_299020	61	193	XXCC
	EhRab7H	XP_653414	EHI_005900	198	XXCC	EiRab7H	EIN_288760	46	203	XXCC
	EhRab7I	XP_649308	EHI_189100	205	XXCC	EiRab7I	EIN_196420	66	206	XCCX
Rab8	EhRab8A	XP_653051	EHI_199820	200	XXCC	EiRab8A	EIN_252640	48	202	XXCC
	EhRab8B	XP_652309	EHI_127380	208	XXCC	EiRab8B	EIN_149010	67	207	XXCC
Rab11	EhRab11A	XP_647948	EHI_005460	208	XXCC	EiRab11A	EIN_165880	82	208	XXCC
	EhRab11B	XP_652776	EHI_107250	212	XXCC	EiRab11B	EIN_108540	74	213	XXCC
	EhRab11C	XP_649609	EHI_161030	213	XXCC	EiRab11C	EIN_014150	71	222	XXCC
	EhRab11D	XP_652598	EHI_056100	214	XCXC	EiRab11D	EIN_050950	65	211	XXCC
II. Rab conserved in Entamoeba										
RabA	EhRabA	XP_652258	EHI_168600	199	XCXC	EiRabA	EIN_280980	85	198	XCXC
RabB	EhRabB	XP_652994	EHI_181240	193	XXCC	EiRabB	EIN_110330	69	198	XXCC
RabC	EhRabC1	XP_656355	EHI_153690	205	XXCC	EiRabC1	EIN_058650	81	198	XXCC
	EhRabC2	XP_653593	EHI_045550	207	XXCC	EiRabC2	EIN_094390	81	206	XXCC
	EhRabC3	XP_652352	EHI_143650	209	XXCC	EiRabC3A	EIN_093190	89	207	XXCC
						EiRabC3B	EIN_089560	54	213	XXCC
	EhRabC4	XP_656897	EHI_096220	204	XXCC	EiRabC4	EIN_072390	57	200	XXCC
	EhRabC5	XP_654231	EHI_122730	204	XXCC	EiRabC5	EIN_014860	73	204	XXCC
	EhRabC6	XP_654710	EHI_194280	195	XXCC					
	EhRabC7	XP_652882	EHI_079890	196	XXCC	EiRabC7	EIN_217920	70	201	XXCC
	EhRabC8	XP_651035	EHI_170390	196	XXCC	EiRabC8	EIN_168870	61	190	XXCC
RabD	EhRabD1	XP_652887	EHI_059670	751	XXCC	EiRabD	EIN_184580	61	744	XXCC
	EhRabD2	XP_655208	EHI_164900	265	XXCC					
RabF	EhRabF1	XP_651799	EHI_129740	203	CXXX	EiRabF1	EIN_239370	68	201	CXXX
	EhRabF2	XP_651513	EHI_182030	194	XXCC	EiRabF2	EIN_106040	61	192	XXCC
	EhRabF3	XP_655210	EHI_164880	191	XXCC	EiRabF3	EIN_112540	70	188	XXCC
	EhRabF4	XP_654217	EHI_122870	191	XXCC	EiRabF4	EIN_239300	65	192	XXCC
	EhRabF5	XP_656060	EHI_117960	197	XXXC	EiRabF5	EIN_228360	85	196	XXXC
RabH	EhRabH1	XP_657074	EHI_133100	209	XCXC	EiRabH	EIN_156660	78	217	XXCC
	EhRabH2[a]	XP_654758	EHI_128180	209	XCXC					
RabI	EhRabI1	XP_655925	EHI_177550	202	XCXC	EiRabI	EIN_014210	65	204	XXCC
	EhRabI2	XP_654235	EHI_053420	214	XCXC					
RabK	EhRabK1	XP_652298	EHI_024680	213	XXCC	EiRabK1	EIN_311490	81	210	XXCC
	EhRabK2	XP_649362	EHI_040450	210	XXCC	EiRabK2	EIN_243000	65	200	XXCC
	EhRabK3	XP_651827	EHI_082550	234	XXCC					
	EhRabK4	XP_648284	EHI_128110	243	XXCC	EiRabK4	EIN_059050	40	227	XXCC
	EhRabK5[a]	XP_655343	EHI_012380	240	XXCC	EiRabK5	EIN_028700	47	226	XXCC

RabL	EhRabL1	XP_651210	EHI_169090	207	XCCX	EiRabL1	EIN_081690	55	202	XXCC
	EhRabL2	XP_648952	EHI_069500	257	XCCX	EiRabL2	EIN_061000	52	210	XCCX
RabM	EhRabM1	XP_652833	EHI_005010	212	XXCC	EiRabM1	EIN_054310	73	213	XXCC
	EhRabM2	XP_652253	EHI_004380	204	XXCC					
	EhRabM3	XP_651723	EHI_068230	205	XXCC	EiRabM3	EIN_052610	79	174	XXCC
RabN	EhRabN1	XP_652702	EHI_048250	202	XCXX	EiRabN1	EIN_136950	71	201	CXXX
	EhRabN2	XP_649426	EHI_097650	199	XXXC	EiRabN2	EIN_054510	68	199	XXXC
RabP	EhRabP1	XP_651771	EHI_114210	204	CXXX	EiRabP	EIN_298880	59	205	CXXX
	EhRabP2	XP_656067	EHI_117890	204	CXXX					
RabX1	EhRabX1	XP_650791	EHI_017740	191	XXCC	EiRabX1A	EIN_299880	49	167	–
						EiRabX1B	EIN_111560	53	190	XXCC
RabX2	EhRabX2	XP_650041	EHI_001870	205	XXCC	EiRabX2A	EIN_134920	57	193	–
						EiRabX2B	EIN_099000	64	186	CXXX
RabX3	EhRabX3	XP_655050	EHI_014220	202	XXXC	EiRabX3[c]	EIN_135850	47	340	–
RabX4	EhRabX4	XP_651716	EHI_100090	195	XXCX	EiRabX4	EIN_240170	44	191	XXCX
RabX5	EhRabX5	XP_657472	EHI_148660	217	XXXC					
RabX6	EhRabX6	XP_652555	EHI_008350	201	CXXX	EiRabX6	EIN_123740	54	191	CXXX
RabX7	EhRabX7	XP_654103	EHI_118920	197	CXXX	EiRabX7	EIN_186210	47	204	CXXX
RabX8	EhRabX8	XP_649911	EHI_178040	210	CCXX					
RabX9	EhRabX9	XP_654197	EHI_140770	183	XXCC	EiRabX9	EIN_243270	45	190	XXCC
RabX10	EhRabX10	XP_656920	EHI_096440	189	CCXXX	EiRabX10	EIN_160760	45	193	CCXXX
RabX11	EhRabX11	XP_655922	EHI_177520	210	XXCC	EiRabX11A	EIN_014910	84	209	XXCC
						EiRabX11B	EIN_059070	77	209	XXCC
						EiRabX11C	EIN_092300	44	205	–
RabX12	EhRabX12	BAD82860	EHI_021210	199	XXCC	EiRabX12	EIN_252860	51	209	XXCC
RabX13	EhRabX13	XP_653656	EHI_065790	208	XXCC					
RabX14	EhRabX14	XP_657126	EHI_053150	354	XXCC	EiRabX14A	EIN_260390	42	228	XXCC
						EiRabX14B	EIN_147580	46	354	XXCC
RabX15	EhRabX15	XP_649287	EHI_177390	193	XXCC	EiRabX15	EIN_238750	65	192	XXCC
RabX16	EhRabX16	XP_655529	EHI_131170	204	XXCC	EiRabX16	EIN_051300	47	214	XXCC
RabX17	EhRabX17	XP_656536	EHI_042250	201	CXXX	EiRabX17A	EIN_072650	68	197	CXXX
						EiRabX17B	EIN_212470	57	197	CXXX
						EiRabX17C	EIN_107380	51	208	CCXXX
RabX18	EhRabX18A	XP_649285	EHI_145720	196	CXXX					
	EhRabX18B[a]	XP_001913559	EHI_177410	194	CXXX					
			EHI_008640							
RabX19	EhRabX19	XP_654968	EHI_183080	207	XXCC	EiRabX19	EIN_288570	46	226	XXCC
RabX20	EhRabX20	XP_652547	EHI_003020	190	XXCC					
RabX21	EhRabX21	XP_650747	EHI_021480	212	CXXXXX					
RabX22	EhRabX22A	XP_655103	EHI_157890	197	XXCC	EiRabX22A	EIN_134610	68	197	XXCC
	EhRabX22B[a]	XP_655064	EHI_014060	197	XXCC	EiRabX22B	EIN_075970	65	184	XXCC
						EiRabX22C	EIN_136400	62	197	XXCC
RabX23	EhRabX23	XP_650671	EHI_107140	187	XXCC	EiRabX23	EIN_241550	76	202	XXCC
RabX24	EhRabX24	XP_656866	EHI_038680	203	XXCC					
RabX25	EhRabX25	XP_653064	EHI_010660	192	XXCC	EiRabX25	EIN_243640	64	189	XXCC
RabX26	EhRabX26	XP_657341	EHI_151610	202	XXCC	EiRabX26	EIN_224230	50	198	XXCC
						EiRabX26B	EIN_060100	40	201	XCXC
RabX27	EhRabX27	XP_650814	EHI_158170	203	CXXX					
RabX28	EhRabX28	XP_647919	EHI_123220	186	CXXX					
RabX29	EhRabX29	XP_656310	EHI_184670	194	CXXX	EiRabX29	EIN_051680	64	198	CXXX
RabX30	EhRabX30	XP_651921	EHI_082230	183	CXXX	EiRabX30	EIN_148610	54	210	CXXX
			EHI_012030							
RabX31	EhRabX31	XP_648905	EHI_040310	194	XXCC	EiRabX31A	EIN_127810	70	189	XXCC
						EiRabX31B	EIN_262240	62	191	XXCC
						EiRabX31C	EIN_191990	42	170	XCXC
						EiRabX31D	EIN_197670	43	170	XCXC
RabX32	EhRabX32	XP_651095	EHI_079230	203	CXXXXX					
RabX33	EhRabX33A	XP_655812	EHI_083390	240	CCXXX					
	EhRabX33B[a]	XP_001914333	EHI_135940	248	CCXXX					

(continued on next page)

Table 1 (*continued*)

Rab subfamily	*Entamoeba histolytica*					*Entamoeba invadens*				
	EhRab isotype	Accession number	ID number	Protein length	C-terminal peptides	EiRab isotype	ID number	% Identity to Eh homologue	Protein length	C-terminal peptides
RabX34	EhRabX34	XP_650332	EHI_114640	200	CXXX	EiRabX34A	EIN_281740	68	204	CXXX
						EiRabX34B	EIN_202640	63	200	CXXX
RabX35	EhRabX35	XP_649164	EHI_130670	195	XXCC	EiRabX35	EIN_156720	52	197	XXCC
RabX36	EhRabX36	XP_657040	EHI_110300	203	–					
RabX37	EhRabX37[a]	XP_652737	EHI_048720	184	XCXX					
RabX38	EhRabX38[a]	XP_656081	EHI_118280	202	CCCXXX					
RabX39	EhRabX39[a]	XP_649044	EHI_094110	180	XXCC	EiRabX39	EIN_238590	44	198	XXCC
RabX40	EhRabX40[a]	XP_657549	EHI_027640	189	–	EiRabX40	EIN_105380	63	189	–
RabX41	EhRabX41[a]	XP_001913412	EHI_051090	189	CXXX	EiRabX41	EIN_186350	52	191	CXXX
RabX42	EhRabX42[a]	XP_651849	EHI_040330	180	CXXX					
III. Rab specific to E. histolytica										
RabX5	EhRabX5	XP_657472	EHI_148660	217	XXXC					
RabX8	EhRabX8	XP_649911	EHI_178040	210	CCXX					
RabX13	EhRabX13	XP_653656	EHI_065790	208	XXCC					
RabX18	EhRabX18A	XP_649285	EHI_145720	196	CXXX					
	EhRabX18B[a]	XP_001913559	EHI_177410	194	CXXX					
			EHI_008640							
RabX20	EhRabX20	XP_652547	EHI_003020	190	XXCC					
RabX21	EhRabX21	XP_650747	EHI_021480	212	CXXXXX					
RabX24	EhRabX24	XP_656866	EHI_038680	203	XXCC					
RabX27	EhRabX27	XP_650814	EHI_158170	203	CXXX					
RabX28	EhRabX28	XP_647919	EHI_123220	186	CXXX					
RabX32	EhRabX32	XP_651095	EHI_079230	203	CXXXXX					
RabX33	EhRabX33A	XP_655812	EHI_083390	240	CCXXX					
	EhRabX33B[a]	XP_001914333	EHI_135940	248	CCXXX					
RabX36	EhRabX36	XP_657040	EHI_110300	203	–					
RabX37	EhRabX37[a]	XP_652737	EHI_048720	184	XCXX					
RabX38	EhRabX38[a]	XP_656081	EHI_118280	202	CCCXXX					
RabX42	EhRabX42[a]	XP_651849	EHI_040330	180	CXXX					
IV. Rab specific to E. invadens										
RabZ1						EiRabZ1	EIN_050800		204	XXCC
RabZ2						EiRabZ2A	EIN_289320		200	CXXX
						EiRabZ2B	EIN_285540		198	CXXX
RabZ3						EiRabZ3	EIN_192430		205	XXCC
RabZ4						EiRabZ4A	EIN_297180		205	CXXX
						EiRabZ4B	EIN_234530		195	CXXX
RabZ5						EiRabZ5	EIN_039070		203	XXCC
RabZ6						EiRabZ6	EIN_051060		187	XXCC
RabZ7						EiRabZ7	EIN_058330		207	XXCC
RabZ8						EiRabZ8A	EIN_270650		191	CXXX
						EiRabZ8B	EIN_261500		150 (partial)	
RabZ9						EiRabZ9	EIN_281720		208	XXCC
RabZ10						EiRabZ10	EIN_105040		234	CCXXC
RabZ11						EiRabZ11	EIN_256390		207	CXXX
RabZ12						EiRabZ12	EIN_038850		207	CCXX
RabZ13						EiRabZ13	EIN_016980		198	XXCC
RabZ14						EiRabZ14	EIN_061010		147 (partial)	–
RabZ15						EiRabZ15	EIN_050890		212	CXXX
RabZ16						EiRabZ16	EIN_071820		195	CXXX
RabZ17						EiRabZ17	EIN_200260		181	CXXX
RabZ18						EiRabZ18	EIN_020600		204	XCCX
RabZ19						EiRabZ19	EIN_017280		200	XXCC
RabZ20						EiRabZ20	EIN_238400		184	CXXC

Rab21	EiRab21	EIN_089250 EIN_026250 EIN_169660 EIN_169890	201	CXXX	
Rab22	EiRabZ22	EIN_165400	213	CXXXXXXX	
Rab23	EiRabZ23	EIN_155360	200	-	
Rab24	EiRabZ24	EIN_055510	230	CXXX	
Rab25	EiRabZ25	EIN_111890	204	XXCC	
Rab26	EiRabZ26	EIN_244150	184	CXXX	

The annotations of *E. histolytica* Rabs are based on a previous publication (Saito-Nakano et al., 2005). The annotations of *E. invadens* Rabs were made on the basis of their percentage identity to the closest *E. histolytica* homologue and by phylogenetic inferences (Fig. 1).

[a] Newly found *E.histolytica* Rab genes in this study.

[b] 32% homology to EhRab21.

[c] EiRabX3 contains two GTPase domains.

2. Methods

2.1. Survey of Rab GTPases in the E. invadens and E. histolytica genome databases

Nucleotide and protein sequences of *S. cerevisiae* and *H. sapiens* Rabs were retrieved from GenBank, National Center of Biotechnology Information (NCBI). For the accession numbers of these proteins, see (Pereira-Leal and Seabra, 2001). We searched the *E. invadens* genome database (http://pathema.jcvi.org/cgi-bin/Entamoeba/PathemaHomePage.cgi) using all yeast and human Rab protein as queries by BLASTP. The *E. invadens* genome database was also searched by BLASTP using EiRab1A as a query. All potential small GTPase genes were further examined by BLASTP analysis against the human database at NCBI; *E. invadens* entries that showed the highest homology to Rab from *Entamoeba* or other organisms were considered to be *E. invadens* Rabs. The *E. histolytica* genome database (release 7.0) at Pathema Bioinformatics Resource Center (http://pathema.jcvi.org/Pathema/) was also searched and 11 previously unannotated *E. histolytica* Rab genes were identified. One hundred and twenty-one *E. invadens* and 11 newly found *E. histolytica* small GTPases were manually inspected to verify the presence of three GTP-binding consensus sequences (GDXXVGKT, DTAGQE, and GNKXD) and five additional conserved regions that are specific to the Rab family (IGVDF, KLQIW, RFRSIT, YYRGA, and LVYDIT) (Pereira-Leal and Seabra, 2000). One hundred and two *E. histolytica* and 121 *E. invadens* putative Rabs were designated according to the previous nomenclature (Saito-Nakano et al., 2005).

2.2. Phylogenetic analysis

Highly conserved domains stretching from the first to the third GTP-binding consensus regions of *E. histolytica*, *E. invadens*, *S. cerevisiae*, and *H. sapiens* Rab proteins were aligned using the CLUSTAL W program version 1.81 (Thompson et al., 1994) with default parameters. Alignments were manually inspected and corrected, and gaps were removed. Finally, 110 unambiguously aligned sites were selected for phylogenetic analysis by the neighbor-joining method (Saitou and Nei, 1987). Phylogenetic trees were drawn using TreeView software (http://taxonomy.zoology.gla.ac.uk/rod/rod.html).

3. Results and discussion

3.1. Annotation and conservation of E. invadens Rabs

3.1.1. Identification of new E. histolytica Rabs

We previously annotated 91 Rab genes in *E. histolytica* using the *E. histolytica* genome database available at TIGR (as of February 24, 2005; Saito-Nakano et al., 2005). A thorough search of the latest genome database at Pathema (version 7.0) identified 11 additional Rab genes; accordingly the current number of *E. histolytica* Rab genes increased to 102 (Table 1). The newly identified genes were annotated as RabH2, K5, X18B, X22B, X33B, and X37–42 (Table 1).

3.1.2. Assignment of E. invadens Rabs

We identified 121 putative Rab genes in the *E. invadens* genome database at Pathema. The number of *E. invadens* Rab genes was 20% higher than that of *E. histolytica*. *E. invadens* Rab entries were grouped based on their similarity to the corresponding *E. histolytica* homologues and also by phylogenetic inference (Table 1 and Fig. 1). Among the ubiquitous Rabs conserved in eukaryotes (Rab1~21), all isotypes of Rab1/8, 2, 5, 7, and 11 subfamilies that are present in *E. histolytica* are conserved in *E. invadens*, with the

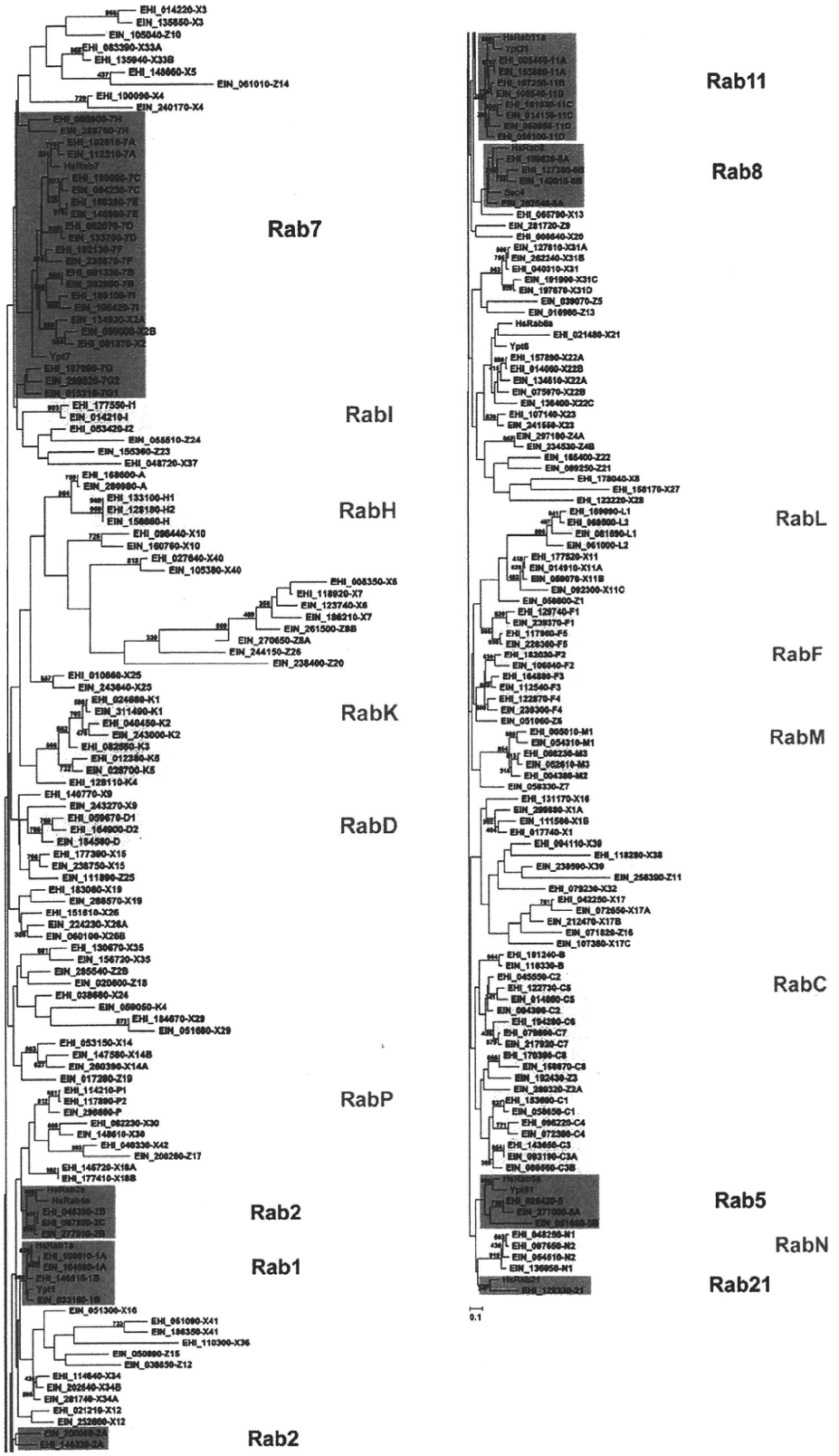

Fig. 1. Phylogenetic analysis of Rab proteins from *E. histolytica*, *E. invadens*, yeast and humans. Phylogenetic analysis of Rab genes from *E. histolytica*, *E. invadens*, yeast, and humans was performed using CLUSTAL W. Trees were drawn using TreeView. The numbers at the nodes represent bootstrap values for 1000 iterations shown in percentages. Yeast and human Rabs are indicated by Ypt and HsRab, respectively. Rabs from *E. histolytica* and *E. invadens* are indicated with their identification number (Table 1; starting with EHI or EIN for *E. histolytica* or *E. invadens* entries, respectively) followed by the subfamily name and number in its abbreviated form. Subfamilies that revealed significant homology (>40% identity) to yeast and human (e.g., Rab5) are shown in dark shaded boxes, while *Entamoeba*-specific subfamilies that contain multiple isotypes are shown in light shaded boxes. The scale bar indicates 0.1 substitutions at each amino acid.

exception of Rab2C. The relative proportion of ubiquitous Rabs conserved in eukaryotes (Rab1~21), *Entamoeba*-specific (i.e., conserved in the two *Entamoeba* species, but not present in other eukaryotes) Rabs (RabA~Z), and species-specific Rabs are similar between *E. histolytica* and *E. invadens* (Fig. 2).

3.1.3. Rabs conserved between E. histolytica and E. invadens

Some Rab subfamilies or isotypes consist of different numbers of isotypes or subisotypes in *E. histolytica* and *E. invadens* (Table 2). Eighty-five percent of Rabs that form subfamilies (e.g., RabC) are conserved (Table 1), suggesting the shared house-keeping roles of these Rab subfamilies in *Entamoeba*. The only exceptions are the RabX18 and RabX33 subfamilies that consist of two isotypes in *E. histolytica*, but are not conserved in *E. invadens*. Conversely, 38% of the solitary (i.e., not forming a subfamily) Rabs are not conserved in *E. invadens*.

3.1.4. Rabs specific to E. histolytica or E. invadens

Among Rab proteins conserved in eukaryotes (Rab1~21), *E. invadens* has additional isotypes of Rab5 and Rab7G, EiRab5B and EiRab7G2, respectively. *E. histolytica* has one each of EhRab5 and EhRab21 that are categorized into the Rab5/Rab21 group (Pereira-Leal and Seabra, 2001). While two EiRab5 isotypes show a 50–83% identity to EhRab5, they show only a 32–33% identity to EhRab21, and were thus annotated as a Rab5 isotype. Phylogenetic analysis (Fig. 1) also supported this annotation.

The number of isotypes and subisotypes in 12 subfamilies and isotypes (Rab5B, 7G2, C3, X1B, X2B, X11B–C, X14B, X17B–C, X22C, X26B, X31B–D, and X34B) is higher in *E. invadens* than in *E. histolytica* (Table 2). In addition, 29 *E. invadens* Rabs (EiRabZ1–26) that show low (<40%) similarity to *E. histolytica* Rabs were discovered and considered to have independently evolved in *E. invadens*. Conversely, homologues corresponding to 26 *E. histolytica* Rabs were not identified in the current *E. invadens* database; however, the lack of these Rabs in *E. invadens* must be confirmed due to the lower coverage of the *E. invadens* genome.

3.2. Review of the demonstrated functions of Rabs in Entamoeba

Although several previous proteomic and transcriptomic studies (see below) suggested that a few dozens of Rab genes/proteins are involved in important biological processes, such as stress response, pathogenesis, and stage conversion, these Rab genes were not discussed. This is partly due to the lack of proper annotation of *Entamoeba* Rab genes at the time of publication. In this section, we summarize the current understanding of the reported functions of Rabs, and also review the previous transcriptomic and proteomic studies that indicate the roles of Rab genes in stress response, pathogenesis, and stage conversion.

Table 2
Rab subfamilies and isotypes that vary in number between *E. histolytica* and *E. invadens*. Seventeen Rab families that have different numbers of isotypes and two isotypes (EhRab7G and EhRabC3) that are encoded by two independent genes are shown.

Rab subfamily/isotype	Number of Rab isotypes	
	E. histolytica	*E. invadens*
Rab2	3	2
Rab5	1	2
Rab7G	1	2
RabC3	1	2
RabD	2	1
RabH	2	1
RabI	2	1
RabK	5	4
RabM	3	2
RabP	2	1
RabX1	1	2
RabX2	1	2
RabX11	1	3
RabX14	1	2
RabX17	1	3
RabX22		3
RabX26	1	2
RabX31	1	4
RabX34	1	2

3.2.1. Demonstrated functions of E. histolytica Rabs

Among all annotated Rabs, there are only a dozen for which their localization, function, or both have been demonstrated. Among the multiple EhRab7 isotypes, EhRab7B is involved in lysosome biogenesis (Fig. 3; Saito-Nakano et al., 2007), while EhRab7A is involved in the targeting of hydrolases to lysosomes (Nakada-Tsukui et al., 2005; Saito-Nakano et al., 2007). EhRab7A, together with EhRab5, also coordinately regulates the formation and matu-

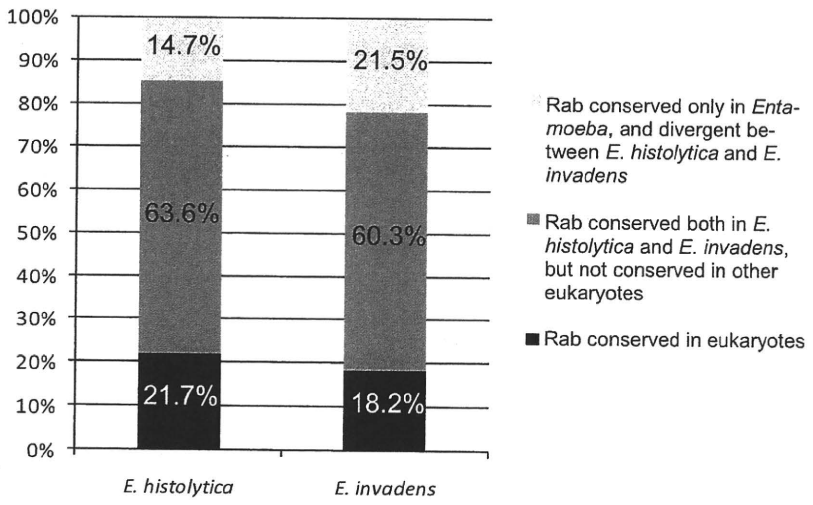

Fig. 2. Percentages of conserved and genus- or species-specific Rab genes in *E. histolytica* and *E. invadens*. Percentage of Rab genes conserved in eukaryotes (Rab1~21, black bars), Rab genes conserved in *E. histolytica* and *E. invadens*, but not conserved in other eukaryotes (RabA~Z, dark shaded bars), and Rab genes conserved only in *Entamoeba* and divergent between *E. histolytica* and *E. invadens* (light shaded bars).

ration of the prephagosomal vacuole (PPV), a unique organelle in *E. histolytica* that is formed during phagocytosis, and is likely to be involved in the processing, activation, or storage of hydrolases that are transported to the phagosome (Saito-Nakano et al., 2004). *E. histolytica*-specific EhRabA was initially suggested to be involved in motility and polarization (Welter et al., 2005), and has been recently shown to be involved in the transport of the Gal/GalNAc-specific lectin (Welter and Temesvari, 2009). EhRab11A was reported to be recruited to the cell surface by iron or serum starvation, and was suggested to be involved in encystation (McGugan and Temesvari, 2003). In contrast, EhRab11B is involved in cysteine protease secretion, and its overexpression enhanced the secretion of cysteine protease (Mitra et al., 2007).

The proteomic analysis of phagosomes isolated from *E. histolytica* trophozoites revealed a panel of phagosome-associated Rabs (Fig. 3; Marion et al., 2005; Okada et al., 2005, 2006). Among the phagosome-associated Rabs, RabD2, P2, and X37 are not conserved in *E. invadens* (Table 1). Interestingly, EhRabD2 and EhRabX37 were expressed only in trophozoites, but not in cysts; their expression was also downregulated during oxidative stress (Table 3, see below). The role of these Rabs appears to be specific to *E. histolytica*, and may be associated with virulence. It needs to be confirmed by proteomic analysis of isolated *E. invadens* phagosomes whether Rab proteins and other phagosome proteins are shared by both species.

3.2.2. Stress- or infection-induced regulation of Rab gene expression

Previous transcriptomic studies indicated that several Rab genes are transcriptionally regulated during stress, stage conversion, and animal infection (Table 3). Incubation of trophozoites at 42 °C for 1 h caused the upregulation of the EhRab7A gene by 2-fold (MacFarlane et al., 2005). It was also shown that the levels

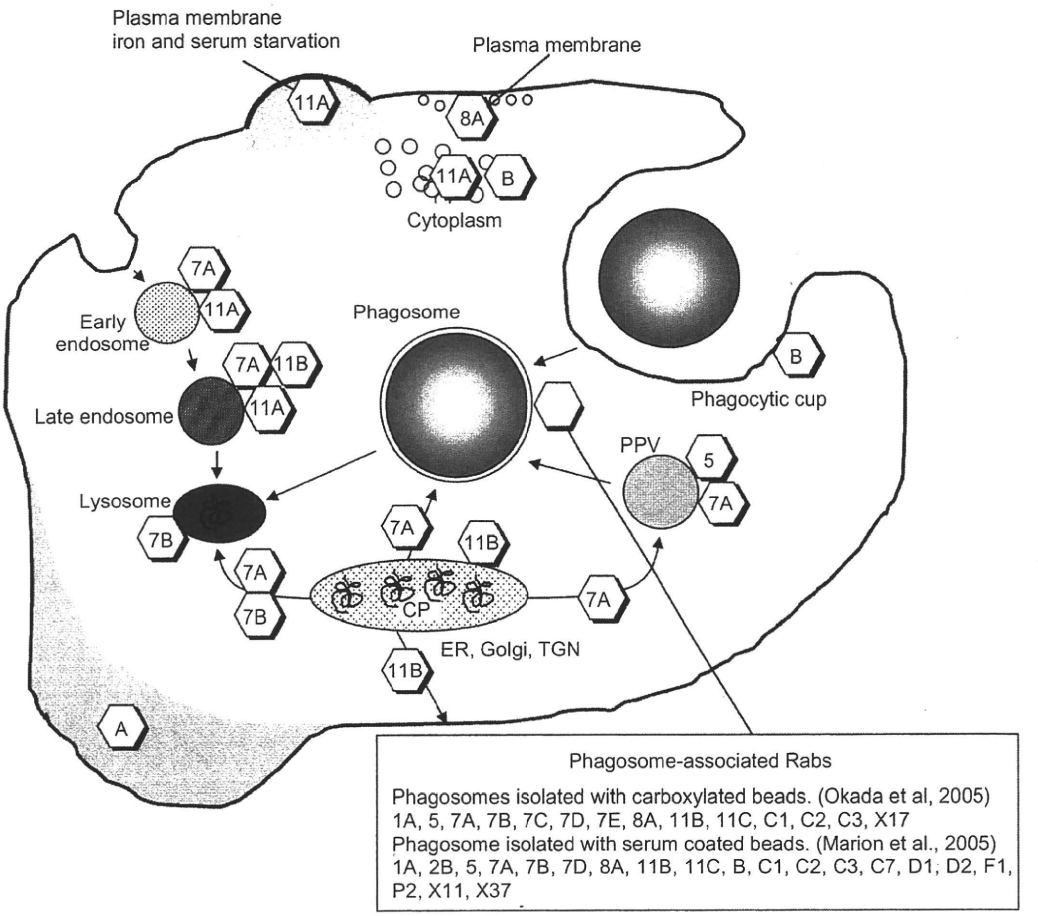

Fig. 3. Demonstrated and presumed localization and function of *E. histolytica* Rabs. Summarized scheme of the localization and function of selected *E. histolytica* Rab proteins is shown based on previous publications. (1) Endosomes: EhRab7A, EhRab11A, and EhRab11B were demonstrated to be localized to endosomes by immunofluorescence assay (EhRab7A and EhRab11B), or immunoblot analysis using iron-dextran-containing endosomes isolated using magnetic separation (EhRab7A and EhRab11A) (Temesvari et al., 1999; Saito-Nakano et al., 2004; Nakada-Tsukui et al., 2005; Mitra et al., 2007). EhRab11A was not demonstrated to be located on endosomes by immunofluorescence, but was suggested to be translocated to the cell surface upon iron and serum starvation or encystation (McGugan and Temesvari, 2003). (2) Phagosomes: EhRabB was localized to the phagocytic cup (Rodriguez et al., 2000). Phagosome-associated Rab proteins, demonstrated by proteomic analysis of isolated phagosomes using carboxylated beads (Okada et al., 2005) or serum-coated beads (Marion et al., 2005), are found in the islet. All Rab proteins detected at various time points of phagocytosis in different strains are listed. (3) Prephagosomal vacuoles (PPV): PPV were reported to be a reservoir of cysteine proteases and other digestive enzymes transported to the phagosome, and EhRab5 and EhRab7A were localized to PPV (Saito-Nakano et al., 2004). (4) Lysosomes: EhRab7A is involved in the transport of cysteine proteases to phagosomes and lysosomes, and a partial association of EhRab7A with lysosomes was observed (Nakada-Tsukui et al., 2005; Saito-Nakano et al., 2007). EhRab11B was suggested to be involved in the transport of cysteine proteases (Mitra et al., 2007), although its exact localization remains unknown. EhRab7B was present in lysosomes and involved in lysosome biogenesis, together with EhRab7A (Saito-Nakano et al., 2007). (5) Secretory vesicles or post-Golgi compartments: EhRab8 showed peripheral dotted localization underneath the plasma membrane, and was suggested to be involved in secretion (Juarez et al., 2001). (6) Unknown compartments in the cytoplasm: EhRabB revealed a punctate dotted localization throughout the cytoplasm, but its exact localization remains to be determined (Rodriguez et al., 2000). EhRabA was localized to the leading edge of the cell and was presumed to regulate cell motility and polarization (Welter and Temesvari, 2004; Welter et al., 2005). Furthermore, the overexpression of dominant negative EhRabA caused an alteration of ER morphology and the localization of the Gal/GalNAc-specific lectin (Welter and Temesvari, 2009).

Table 3
Rab genes that are differentially expressed.

Rab gene	Fold change	Up/down	Condition/stage/strain	Method[a]	Reference[b]
Ehrab5	3.62	Down	Cyst (vs. trophozoite)	D	a
	3.2	Down	*E. dispar* (vs. *E. histolytica*)	D	b
Ehrab7A	2	Up	Heat shock[c]	D	c
Ehrab7D	25.37	Up	Avirulent HM-1 (vs. virulent HM-1)	D	d
	3.55	Down	Cyst (vs. trophozoite)	D	a
Ehrab7E	62	Up	Avirulent HM-1 (vs. virulent HM-1)	D	d
Ehrab7F	4.8	Down	Oxidative stress[e], HM-1	D	e
	4.4	Down	NO stress[f]	D	
Ehrab7G	14.5	Up	Avirulent HM-1 (vs. virulent HM-1)	D	d
Ehrab11A	4.23	Down	Cyst (vs. trophozoite)	D	a
Ehrab11B	4.55	Down	Cyst (vs. trophozoite)	D	a
Ehrab11D	8.43	Down	Cyst (vs. trophozoite)	D	a
EhrabB	5	Up	Heat shock[d]	P	f
	3.32	Down	Cyst (vs. trophozoite)	D	a
EhrabC1	2.2	Down	Cyst (vs. trophozoite)	D	a
EhrabC2	2.2	Down	NO stress[f]	D	e
EhrabC5	3.66	Down	Cyst (vs. trophozoite)	D	a
EhrabC6	6.15	Down	Cyst (vs. trophozoite)	D	a
EhrabD2	5.52	Down	Cyst (vs. trophozoite)	D	a
	2.8	Down	Oxidative stress[e], HM-1	D	e
EhrabH1	3.41	Down	Cyst (vs. trophozoite)	D	a
EhrabI1	3.56	Up	Oxidative stress[e], HM-1	D	e
	3.5	Up	NO stress[f]	D	
EhrabK2	7.14	Down	Cyst (vs. trophozoite)	D	a
EhrabL1	2.7	Down	NO stress[f]	D	e
EhrabM1	6.7	Up	Cyst (vs. trophozoite)	D	a
	2	Up	Oxidative stress[e], HM-1	D	e
EhrabM2	3.65	Down	Cyst (vs. trophozoite)	D	a
EhrabNI	4.1	Up	Cyst (vs. trophozoite)	D	a
EhrabX6	4.76	Down	*E. dispar* (vs. *E. histolytica*)	D	b
EhrabX13	2	Down	*E. dispar* (vs. *E. histolytica*)	D	b
EhrabX14	2.95	Up	Day 1 of intestinal challenge	D	g
	2.86	Up	Day 29 of intestinal challenge	D	
EhrabX15	3	Up	NO stress[f]	D	e
EhrabX19	5.1	Down	NO stress[f]	D	e
EhrabX31	2	Up	Oxidative stress[e], Rhaman	D	e
EhrabX32	2.7	Up	NO stress[f]	D	e
EhrabX35	2.3	Up	Oxidative stress[e], Rhaman	D	e
	2	Up	NO stress[f]	D	
EhrabX37	3.84	Down	Cyst (vs. trophozoite)	D	a
EhrabX42	2.43	Down	NO stress[f]	D	e

[a] D, DNA microarray; P, real-time PCR.
[b] (a) Ehrenkaufer et al. (2007), (b) MacFarlane and Singh (2006), (c) MacFarlane et al. (2005), (d) Biller et al. (2010), (e) Vicente et al. (2009), (f) Romero-Diaz et al. (2007), (g) Gilchrist et al. (2006).
[c] 42 °C, 1 h.
[d] 42 °C, 5 h.
[e] 1 mM H_2O_2, 1 h.
[f] HM-1, 200 μM dipropylenetriamine (DPTA)-NONNate, 1 h.

of the EhRabB transcript increased by 5-fold after incubation at 42 °C for 5 h (Romero-Diaz et al., 2007). It was suggested that the putative heat shock elements (HSE) upstream of the EhRabB gene are involved in the regulation of EhRabB (Romero-Diaz et al., 2007). It was also shown that incubation of trophozoites from the HM-1 and Rhaman strains with hydrogen peroxide or the nitric oxide donor dipropylenetriamine-NONOate (DPTA), caused a 4-fold upregulation of EhRabI1, and a 4.4–4.8-fold downregulation of EhRab7F (Vicente et al., 2009). Since these Rabs appeared to be regulated in a similar way by hydrogen peroxide and nitric oxide, common regulator(s) and pathway(s) may be involved in the responses against these stresses. It should be noted that some Rab genes differentially respond to oxidative and nitric oxide stress. For example, EhRabM1 and EhRabX31 were upregulated only by hydrogen peroxide, while EhRabX15, X32, and X35 were upregulated only by DPTA (Vicente et al., 2009). Similarly, EhRabD2 was downregulated by oxidative stress, whereas EhRabC2, L1, and X19 were downregulated by nitric oxide (Vicente et al., 2009). Although the role of these Rabs remains unknown, these findings indicate a possible link between oxidative/nitrosative stress response and membrane trafficking. In addition, it was shown that during mouse intestinal infection, EhRabX14 expression was upregulated on days 1 and 29 post-infection (Gilchrist et al., 2006). These change in expression may also be a consequence of the stress response because amoebae are exposed to reactive oxygen and nitrogen species during host invasion.

3.2.3. Differences in Rab gene expression between *E. histolytica* and *E. dispar*, and between virulent and avirulent *E. histolytica* strains

A comparison of the transcriptome of the non-pathogenic sibling *E. dispar* and *E. histolytica* also revealed that Rab5, X6, and X13 were downregulated in *E. dispar* (MacFarlane and Singh, 2006). Since Rab5 plays a role in the formation of the PPV in *E. histolytica* (Saito-Nakano et al., 2004), the repression of Rab5 expression in *E. dispar* may indicate the suppressed activity of phagocytosis and endocytosis in *E. dispar* (Mitra et al., 2005). Recently, transcriptomic analysis of two HM-1 strains with different abilities to form amoebic liver abscess was reported (Biller et al., 2010). The expression of three Rab7 subfamilies, EhRab7D, 7E, and 7G, was augmented in the avirulent HM-1 strain, obtained

from American Type Culture Collection (ATCC). In contrast, EhRab7D and 7G were poorly transcribed in an independently established attenuated HM-1 strain (Mitra et al., 2006; Saito-Nakano et al., 2007). These data suggest that the expression of individual Rab7 isotypes may be largely affected by subtle changes in the *in vitro* culture conditions.

3.2.4. Regulation of Rab gene expression during stage conversion

Several EhRab genes have been suggested to play a role in the stage conversion of *E. histolytica* (Ehrenkaufer et al., 2007). Transcriptomic analysis of clinical isolates and an attenuated HM-1 strain showed that EhRabM1 and EhRabN1 were expressed 6.7- and 4.1-fold higher in clinical isolates, respectively, than in HM-1 (Table 3). Since the clinical isolates used partially retained an ability to encyst *in vitro*, which attenuated HM-1 strain had lost, these data may indicate that the aforementioned Rabs are likely to be upregulated in the cyst or during encystation. In contrast, Rab5, 7D, 11A, 11B, 11D, B, C1, C5, C6, D2, H1, K2, M2, and X37, were expressed at higher levels in the laboratory strain, which does not encyst, compared to the clinical isolates, suggesting that these Rabs may be upregulated in the trophozoite stage (Ehrenkaufer et al., 2007). EhRabM1 was upregulated in the cyst stage and by oxidative stress, which may suggest a common role of EhRabM1 in stress response and differentiation. It is worth examining whether these changes are found in the cyst-like form of *E. histolytica* induced by oxidative stress (Aguliar-Diaz et al., 2010).

In summary, we proposed the annotation of *E. invadens* and *E. histolytica* Rab genes. Comparison of the Rab repertoire between the two species demonstrated that the majority of Rabs is conserved between the two species, while there are also species-specific Rabs. To understand the individual roles of Rabs, further functional studies are necessary. For instance, comprehensive transcriptomic analysis of Rab genes during the encystation of *E. invadens* should identify stage-specific regulated Rab genes and reveal ubiquitous or species-specific Rab-mediated encystation mechanisms in *Entamoeba*.

Acknowledgments

We thank Lis Caler, Bioinformatics Resource Center, J. Craig Venter Institute for sharing unpublished information of the *E. invadens* genome, and Takashi Makiuchi for his help with the phylogenetic analyses. We thank Eiko Nakasone for her help in the search for Rab genes from *E. invadens*. This work was supported by Creative Scientific Research (18GS0314) from the Japanese Ministry of Education, Science, Culture, Sports, and Technology to T.N., a Grant-in-Aid for Scientific Research from the Japanese Ministry of Education, Culture, Sports, Science, and Technology to T.N. (18GS0314, 18050006, and 18073001), a grant for research on emerging and re-emerging infectious diseases from the Japanese Ministry of Health, Labour, and Welfare, and a grant for research to promote the development of anti-AIDS pharmaceuticals from the Japan Health Sciences Foundation to T.N.

References

Aguliar-Diaz, H., Diaz-Gallardo, M., Laclette, J.P., Carrero, C.J., 2010. In vitro induction of *Entamoeba histolytica* cyst-like structures from trophozoites. PLoS Neglected Tropical Diseases 4, e607.

Biller, L., Davis, P.H., Tillack, M., Matthiesen, J., Lotter, H., Stanley, S.L., Tannich, E., Bruchhaus, I., 2010. Differences in the transcriptome signatures of two genetically related *Entamoeba histolytica* cell lines derived from the same isolate with different pathogenic properties. BMC Genomics 11, 63.

Bourne, H.R., Sanders, D.A., McCormick, F., 1990. The GTPase superfamily: a conserved switch for diverse cell functions. Nature 348, 125–132.

Carlton, J.M., Hirt, R.P., Silva, J.C., Delcher, A.L., Schantz, M., Zhao, Q., Wortman, J.R., Bidwell, S.L., Alsmark, U.C., Besterio, S., Sicheritz-Ponten, T., Noel, C.J., Dacks, J.B., Foster, P.G., Simillion, C., et al., 2007. Draft genome sequence of the sexually transmitted pathogen *Trichomonas vaginalis*. Science 315, 207–212.

Chatterjee, A., Ghosh, S.K., Jang, K., Bullitt, E., Moore, L., Robbins, P.W., Samuelson, J., 2009. Evidence for a "wattle and daub" model of the cyst wall of *Entamoeba*. PLoS Pathogens 5, e1000498.

Ehrenkaufer, G.M., Haque, R., Hackney, J.A., Eichinger, D.J., Singh, U., 2007. Identification of developmentally regulated genes in *Entamoeba histolytica*: insights into mechanisms of stage conversion in a protozoan parasite. Cellular Microbiology 9, 1426–1444.

Eichinger, D., 1997. Encystation of *Entamoeba* parasites. Bioessays 19, 633–639.

Eichinger, D., 2001. Encystation in parasitic protozoa. Current Opinion in Microbiology 4, 421–426.

Gilchrist, C.A., Houpt, E., Trapaidze, N., Fei, Z., Crasta, O., Asgharpour, A., Evans, C., Martino-Catt, S., Baba, D.J., Stroup, S., Hamano, S., Ehrenkaufer, G., Okada, M., Singh, U., Nozaki, T., Mann, B.J., Petri Jr., W.A., 2006. Impact of intestinal colonization and invasion on the *Entamoeba histolytica* transcriptome. Molecular and Biochemical Parasitology 147, 163–176.

Juarez, P., Sanchez-Lopez, R., Stock, R.P., Olvera, A., Ramos, M.A., Alagon, A., 2001. Characterization of the EhRab8 gene, a marker of the late stages of the secretory pathway of *Entamoeba histolytica*. Molecular and Biochemical Parasitology 116, 223–228.

MacFarlane, R.C., Singh, U., 2006. Identification of differentially expressed genes in virulent and nonvirulent *Entamoeba* species: potential implications for amebic pathogenesis. Infection and Immunity 74, 340–351.

MacFarlane, R., Bhattacharya, D., Singh, U., 2005. Genomic DNA microarrays for *Entamoeba histolytica*: applications for use in expression profiling and strain genotyping. Experimental Parasitology 110, 196–202.

Marion, S., Laurent, C., Guillén, N., 2005. Signalization and cytoskeleton activity through myosin IB during the early steps of phagocytosis in *Entamoeba histolytica*: a proteomic approach. Cellular Microbiology 7, 1504–1518.

McGugan Jr., G.C., Temesvari, L.A., 2003. Characterization of a Rab11-like GTPase, EhRab11, of *Entamoeba histolytica*. Molecular and Biochemical Parasitology 129, 137–146.

Mitra, B.N., Yasuda, T., Kobayashi, S., Saito-Nakano, Y., Nozaki, T., 2005. Differences in morphology of phagosomes and kinetics of acidification and degradation in phagosomes between the pathogenic *Entamoeba histolytica* and the non-pathogenic *Entamoeba dispar*. Cell Motility and Cytoskeleton 62, 84–99.

Mitra, B.N., Kobayashi, S., Saito-Nakano, Y., Nozaki, T., 2006. *Entamoeba histolytica*: differences in phagosome acidification and degradation between attenuated and virulent strains. Experimental Parasitology 114, 57–61.

Mitra, B.N., Saito-Nakano, Y., Nakada-Tsukui, K., Sato, D., Nozaki, T., 2007. Rab11B small GTPase regulates secretion of cysteine proteases in the enteric protozoan parasite *Entamoeba histolytica*. Cellular Microbiology 9, 2112–2125.

Nakada-Tsukui, K., Saito-Nakano, Y., Ali, V., Nozaki, T., 2005. A retromerlike complex is a novel Rab7 effector that is involved in the transport of the virulence factor cysteine protease in the enteric protozoan parasite *Entamoeba histolytica*. Molecular Biology of the Cell 16, 5294–5303.

Novick, P., Zerial, M., 1997. The diversity of Rab proteins in vesicle transport. Current Opinion in Cell Biology 9, 496–504.

Nozaki, T., Nakada-Tsukui, K., 2006. Membrane trafficking as a virulence mechanism of the enteric protozoan parasite *Entamoeba histolytica*. Parasitology Research 98, 179–183.

Okada, M., Huston, C.D., Mann, B.J., Petri Jr., W.A., Kita, K., Nozaki, T., 2005. Proteomic analysis of phagocytosis in the enteric protozoan parasite *Entamoeba histolytica*. Eukaryotic Cell 4, 827–831.

Okada, M., Huston, C.D., Oue, M., Mann, B.J., Petri Jr., W.A., Kita, K., Nozaki, T., 2006. Kinetics and strain variation of phagosome proteins of *Entamoeba histolytica* by proteomic analysis. Molecular and Biochemical Parasitology 145, 171–183.

Pereira-Leal, J.B., Seabra, M.C., 2000. The mammalian Rab family of small GTPases: definition of family and subfamily sequence motifs suggests a mechanism for functional specificity in the Ras superfamily. Journal of Molecular Biology 301, 1077–1087.

Pereira-Leal, J.B., Seabra, M.C., 2001. Evolution of the Rab family of small GTP-binding proteins. Journal of Molecular Biology 313, 889–901.

Picazarri, K., Nakada-Tsukui, K., Nozaki, T., 2008. Autophagy during proliferation and encystation in the protozoan parasite *Entamoeba invadens*. Infection and Immunity 76, 278–288.

Rodriguez, M.A., Garcia-Perez, R.M., Garcia-Rivera, G., Lopez-Reyes, I., Mendoza, L., Ortiz-Navarrete, V., Orozco, E., 2000. An *Entamoeba histolytica* rab-like encoding gene and protein: function and cellular location. Molecular and Biochemical Parasitology 108, 199–206.

Romero-Diaz, M., Gomez, C., Lopez-Reyes, I., Martinez, M.B., Orozco, E., Rodriguez, M.A., 2007. Structural and functional analysis of the *Entamoeba histolytica* EhrabB gene promoter. BMC Molecular Biology 8, 82.

Saito-Nakano, Y., Yasuda, T., Nakada-Tsukui, K., Leippe, M., Nozaki, T., 2004. Rab5-associated vacuoles play a unique role in phagocytosis of the enteric protozoan parasite *Entamoeba histolytica*. Journal of Biological Chemistry 279, 49497–49507.

Saito-Nakano, Y., Loftus, B.J., Hall, N., Nozaki, T., 2005. The diversity of Rab GTPases in *Entamoeba histolytica*. Experimental Parasitology 110, 244–252.

Saito-Nakano, Y., Mitra, B.N., Nakada-Tsukui, K., Sato, D., Nozaki, T., 2007. Two Rab7 isotypes, EhRab7A and EhRab7B, play distinct roles in biogenesis of lysosomes and phagosomes in the enteric protozoan parasite *Entamoeba histolytica*. Cellular Microbiology 9, 1796–1808.

Saitou, N., Nei, M., 1987. The neighbor-joining method: a new method for reconstructing phylogenetic trees. Molecular Biology of Evolution 4, 406–425.

Singh, U., Ehrenkaufer, G.M., 2009. Recent insights into *Entamoeba* development: identification of transcriptional networks associated with stage conversion. International Journal of Parasitology 39, 41–47.

Stenmark, H., 2009. Rab GTPases as coordinators of vesicle traffic. Nature Reviews Molecular Cell Biology 10, 513–525.

Takai, Y., Sasaki, T., Matozaki, T., 2001. Small GTP-binding proteins. Physiological Reviews 81, 153–208.

Temesvari, L.A., Harris, E.N., Stanely, S.L., Cardelli, J.A., 1999. Early and late endosomal compartments of *Entamoeba histolytica* are enriched in cysteine proteases, acid phosphatase and several Ras-related Rab GTPases. Molecular and Biochemical Parasitology 103, 225–241.

Thompson, D.J., Higgins, D.G., Gibson, T.J., 1994. CLUSTAL W: improving the sensitivity of program multiple sequence alignment through sequence weighting, positive-specific gap penalties and weight matrix choice. Nucleic Acids Research 22, 4673–4680.

Vicente, J.B., Ehrenkaufer, G.M., Saraiva, L.M., Teixeira, M., Singh, U., 2009. *Entamoeba histolytica* modulates a complex repertoire of novel genes in response to oxidative and nitrosative stresses: implications for amebic pathogenesis. Cellular Microbiology 11, 51–69.

Wang, Z., Samuelson, J., Clark, C.G., Eichinger, D., Paul, J., Van Dellen, K., Hall, N., Anderson, I., Loftus, B., 2003. Gene discovery in the *Entamoeba invadens* genome. Molecular and Biochemical Parasitology 129, 23–31.

Welter, B.H., Temesvari, L.A., 2004. A unique Rab GTPase, EhRabA, of *Entamoeba histolytica*, localizes to the leading edge of motile cells. Molecular and Biochemical Parasitology 135, 185–195.

Welter, B.H., Temesvari, L.A., 2009. Overexpression of a mutant form of EhRabA, a unique Rab GTPase of *Entamoeba histolytica*, alters endoplasmic reticulum morphology and localization of the Gal/GalNAc adherence lectin. Eukaryotic Cell 8, 1014–1026.

Welter, B.H., Powell, R.R., Leo, M., Smith, C.M., Temesvari, L.A., 2005. A unique Rab GTPase, EhRabA, is involved in motility and polarization of *Entamoeba histolytica* cells. Molecular and Biochemical Parasitology 140, 161–173.

International Journal for Parasitology 40 (2010) 833–843

Contents lists available at ScienceDirect

International Journal for Parasitology

journal homepage: www.elsevier.com/locate/ijpara

Members of the *Entamoeba histolytica* transmembrane kinase family play non-redundant roles in growth and phagocytosis

Sarah N. Buss [a,*], Shinjiro Hamano [b], Alda Vidrich [c], Clive Evans [d], Yan Zhang [d], Oswald R. Crasta [d], Bruno W. Sobral [d], Carol A. Gilchrist [e], William A. Petri Jr. [e]

[a] Department of Microbiology, University of Virginia, Charlottesville, VA 22908-1340, USA
[b] Department of Parasitology, Institute of Tropical Medicine (NEKKEN) and the Global COE Program, Nagasaki University, Nagasaki 852-8523, Japan
[c] Digestive Health Center of Excellence, Department of Medicine, University of Virginia, Charlottesville, VA 22908-1340, USA
[d] Virginia Bioinformatics Institute, Blacksburg, Virginia, 24061-0477, USA
[e] Division of Infectious Diseases and International Health, Departments of Internal Medicine, Microbiology and Pathology, University of Virginia, Charlottesville, VA 22908-1340, USA

ARTICLE INFO

Article history:
Received 13 November 2009
Received in revised form 15 December 2009
Accepted 17 December 2009

Keywords:
Entamoeba histolytica
Transmembrane kinase
Phagocytosis
Lectin
Laser-capture microdissection

ABSTRACT

Entamoeba histolytica contains a large and novel family of transmembrane kinases (TMKs). The expression patterns of the *E. histolytica* TMKs in individual trophozoites and the roles of the TMKs for sensing and responding to extracellular cues were incompletely characterised. Here we provide evidence that single cells express multiple TMKs and that TMK39 and TMK54 likely serve non-redundant cellular functions. Laser-capture microdissection was used in conjunction with microarray analysis to demonstrate that single trophozoites express more than one TMK gene. Anti-peptide antibodies were raised against unique regions in the extracellular domains of TMK39, TMK54 and PaTMK, and TMK expression was analysed at the protein level. Flow cytometric assays revealed that populations of trophozoites homogeneously expressed TMK39, TMK54 and PaTMK, while confocal microscopy identified different patterns of cell surface expression for TMK39 and TMK54. The functions of TMK39 and TMK54 were probed by the inducible expression of dominant-negative mutants. While TMK39 co-localised with ingested beads and expression of truncated TMK39 interfered with trophozoite phagocytosis of apoptotic lymphocytes, expression of a truncated TMK54 inhibited growth of amoebae and altered the surface expression of the heavy subunit of the *E. histolytica* Gal/GalNAc lectin. Overall, our data indicates that multiple members of the novel *E. histolytica* TMK family are utilised for non-redundant functions by the parasite.

1. Introduction

Cell surface receptors mediate the response to the environment across all forms of life. In metazoan organisms and plants, transmembrane kinases (TMKs) make up one of the major classes of cell surface receptors, with humans encoding about 80 TMKs (Manning et al., 2002) and *Arabidopsis thaliana* encoding over 400 (Champion et al., 2004; Shiu et al., 2004). The paradigm of receptor-mediated signalling governing cellular responses to environmental cues in plants and metazoa has not been fully extended to protozoa because protozoa have a general paucity of TMKs. However, examples of protozoan TMKs are beginning to be discovered and include nine predicted TMKs in *Dictyostelium discoideum* (Goldberg et al., 2006), 10 potential TMKs in *Trypanosoma brucei* (Parsons et al., 2005), 11 putative TMKs in *Plasmodium* (Ward et al., 2004), 88 predicted TMKs in *Monosiga brevicollis* (King and Carroll, 2001; Manning et al., 2008) and over 90 novel TMKs predicted in the protozoan parasite *Entamoeba histolytica* (Beck et al., 2005). The significance of these proteins remains unclear, as the majority have been characterised by sequence analysis only. A more complete understanding of protozoan TMKs will help define the mechanisms that these organisms use to respond to their environment and may shed light on the evolution of eukaryotic protein kinases.

The large family of novel TMKs identified in the *E. histolytica* genome has proposed roles in both amoebic response to the environment and immune evasion (Beck et al., 2005). *E. histolytica* is the causative agent of amoebiasis, a disease responsible for significant morbidity and mortality worldwide (WHO/PAHO/UNESCO, 1997). The parasite's biphasic life cycle consists of transmissible cysts and replicating trophozoites that colonise the lumen of the large intestine and occasionally invade the mucosa. Trophozoites must survey and adapt to the complex intestinal milieu and evade the immune system, but mechanisms that regulate the parasite's ability to persist for months within its human host remain incompletely understood.

* Corresponding author. Address: Division of Infectious Diseases and International Health, University of Virginia Health System, Carter Harrison Building Room 1711, 345 Crispell Drive, Charlottesville, VA 22908-1340, USA. Tel.: +1 434 924 8189; fax: +1 434 924 0075.
E-mail address: snb4k@virginia.edu (S.N. Buss).

0020-7519/$36.00 © 2010 Australian Society for Parasitology Inc. Published by Elsevier Ltd. All rights reserved.
doi:10.1016/j.ijpara.2009.12.007

In protozoan parasites such as *Giardia lamblia, Plasmodium falciparum* and *T. brucei*, antigenic variation, or the alteration of immunodominant surface antigens, is a common mechanism used to subvert host defences (Adam et al., 1988; Su et al., 1995; Stockdale et al., 2008). The process requires three elements: a large gene family encoding antigenically distinct surface proteins, expression of one variant antigen at a time by a single pathogen and a mechanism to switch the expressed gene (Borst and Genest, 2006). The *E. histolytica* TMKs have been implicated in the process of antigenic variation due to the nature of the gene family, the course of amoebic infection and observations made during transcriptional profiling studies (Beck et al., 2005). Additionally, some *E. histolytica* TMKs share sequence similarity with the variant-specific surface proteins (VSP) that are involved in the process of antigenic variation in *G. lamblia* (Beck et al., 2005).

It is possible that *Entamoeba* trophozoites undergo antigenic variation, as prolonged *E. histolytica* infections do occur (Haque et al., 2002) and antibody mediated protective immunity against *Entamoeba* is incomplete (Haque et al., 2001). However, trophozoites are known to use the process of capping, whereby antibody–antigen complexes are concentrated and released from the cell surface, as a means to avoid immune attack (Calderón et al., 1980). Additionally, amoebic trophozoites directly kill and ingest host cells, providing the organism with another mechanism for immune evasion (Ravdin et al., 1980). Nonetheless, it remains possible that the unusual TMK family may be involved with the process of antigenic variation. Real time PCR analysis of TMK expression by trophozoites during growth in culture revealed temporal changes in expression levels of some TMKs (Beck et al., 2005). As antigenic variation is known to occur without immune pressure (Roberts et al., 1992), the observed changes could be indicative of an antigenic switching event, where the averaging of population data masked expression of a single TMK by each cell.

Changes in TMK expression levels could also indicate that TMKs have specialised functions, as the TMKs have also been proposed to represent a major receptor system used by the cell to sense and respond to extracellular cues. The structural organisation of the *E. histolytica* TMKs suggests that they are type 1 integral membrane proteins, with signal-peptides, receptor-like extracellular domains and intracellular kinase domains, phylogenetically related to both S/T and Y kinases (Beck et al., 2005). When the TMKs were divided into nine sub-groups (A, B_{1-3}, C, D_{1-2}, E and F) based on signature motifs found within the substrate recognition regions of their kinase domains, similarity in the extracellular domains became apparent within sub-groups with respect to the size and the distribution of cysteine-rich motifs, suggesting that TMK sub-groups represent functionally distinct receptor families with sub-family-specific substrates and ligands (Beck et al., 2005). However, only two TMKs have been partially characterised to date: PaTMK (TMK-96, sub-family B_3) is expressed at the cell surface and functions in erythrophagocytosis (Boettner et al., 2008) and members of the B_1 family of TMKs play a role in proliferation and sensitivity to serum-derived growth factors (Mehra et al., 2006).

In this study, we sought to determine whether TMKs represent a gene family that undergoes antigenic variation or are an example of a protozoan TMK family that likely represents a major cell surface receptor system. We used laser-capture microdissection (LCM) and single cell microarray analysis and determined that a single amoeba expresses more than one TMK. To confirm expression of some TMKs at the protein level, anti-peptide antibodies were developed against TMK39 and TMK54. These TMKs were chosen because microarray data previously indicated that the genes were highly transcribed (amongst the TMKs) in both cultured and animal passaged trophozoites (Gilchrist et al., 2006), and TMK39 was identified at an early time point in a phagosomal proteome (Okada et al., 2006). We used the anti-peptide antibodies to stain cells for flow cytometric analysis and determined that the TMKs were homogenously expressed by trophozoites within a population. The antibodies were also used to localise TMK39 and TMK54 to discrete regions of the amoebic plasma membrane. We then utilised a functional genetic approach to demonstrate that TMK39 and TMK54 likely serve non-redundant cellular functions.

2. Materials and methods

2.1. Cultivation of E. histolytica and LCM

E. histolytica trophozoites, strain HM-1:IMSS, were grown axenically at 37 °C in complete TYI-S-33 medium containing 100 U/ml of penicillin and 100 μg/ml streptomycin (Invitrogen, Carlsbad, CA, USA) (Diamond, 1961). For all experiments, trophozoites were harvested during log-phase growth by a 10 min incubation on ice. For LCM analysis, harvested trophozoites were allowed to adhere to PEN foil-coated glass slides specifically designed for laser microdissection (Leica Microsystems, Bannockburn, IL, USA) for 15 min at 37 °C in TYI-S-33 media. Adherent trophozoites were sequentially fixed for 5 min in 70% and 100% ethanol followed by a few dips in xylene to completely dehydrate the samples and air-dried. Subsequently, single cells were captured from the PEN slides using the Leica AS LMD microdissection system (Leica Microsystems, Bannockburn, IL, USA). Captured cells were immediately processed as described below.

2.2. RNA isolation, amplification and microarray hybridization

RNA was purified from a single amoeba using the PicoPure™ RNA Isolation Kit (Molecular Devices, Sunnyvale, CA, USA) and the WT-Ovation™ Pico System (NuGEN, San Carlos, CA, USA) was used for cDNA synthesis and amplification. The quantity of cDNA obtained from one amplification cycle was insufficient for microarray analysis. Therefore one cycle amplified cDNA (1C) was subjected to a second cycle of amplification. Prior to microarray analysis, the linearity of the relationship between 1C and twice amplified cDNA (2C) was validated by quantitative reverse transcription PCR (qRT-PCR) (Section 2.4). 2C from a single cell was used for biotinylated cRNA synthesis. After biotinylation, 2 μg of cRNA was hybridized to the E_his-1a520285 Affymetrix custom array that has been described elsewhere (Gilchrist et al., 2006). The arrays were washed and stained with streptavidin–phycoerythrin (Molecular Probes, Carlsbad, CA, USA), following the standard Affymetrix protocol for eukaryotic targets (http://www.affymetrix.com/support/technical/manual/expression_manual.affx). The arrays were scanned with an Affymetrix Gene Chip scanner 3000 l and Affymetrix® GeneChip® Operating Software (GCOS) (http://www.affymetrix.com/products/software/specific/gcos.affx) was used to determine the detection call (present, marginal, or absent) for each probe set. The experiment was carried out in duplicate. Additionally, raw data from the arrays were normalised at the probe level by the gcRMA algorithm and then log2 transformed (Irizarry et al., 2003). The average log intensity values for all TMKs and for a few reference genes are listed in Supplementary Table S2. The complete microarray data was deposited in NCBI's Gene Expression Omnibus (Barrett et al., 2005) and is accessible through GEO Series accession number GSE19064 (http://www.ncbi.nlm.nih.gov/geo/query/acc.cgi?acc=GSE19064).

2.3. Genome analysis and datasets

The re-annotated *E. histolytica* genome, available at http://pathema.tigr.org, (GenBank accession number AAFB00000000) was used in this analysis.

2.4. qRT-PCR for validation of amplification and microarray

For validation of RNA amplification procedures, RNA from 10^6 *E. histolytica* trophozoites was prepared using the PicoPure™ RNA Isolation Kit and then subjected to either one or two cycles of amplification with the WT-Ovation™ Pico System. Two rounds of amplification yielded approximately 1.67 times more RNA than one round. 1C and 2C were adjusted to the same concentration and qRT-PCR was performed for 10 TMKs (TMK6, 56, 19, 60, 39, 63, 40, 65, 42 and 71) as previously described (Beck et al., 2005). See Supplementary Table S1 for primer sequences and annealing temperatures. The TMK threshold cycles (CTs) for 1C and 2C were then compared. As shown in Supplementary Fig. S1, 1C and 2C yielded similar CT values for all TMKs examined, indicating that the linearity of amplification was maintained throughout the second cycle.

For microarray validation, cDNA was prepared from a single cell as described above. The 2× amplified cDNA was diluted 1:100 with H_2O and qRT-PCR was carried out using iQSYBRGreen super mix (Bio-Rad, Hercules, CA, USA) and previously developed methods (Beck et al., 2005). Supplementary Table S1 lists primer sequences and annealing temperatures. Two "present" and two "absent" transcripts were selected for validation, and as a positive control cDNA was prepared from 10^6 trophozoites.

2.5. Antibodies

Peptides corresponding to amino acids (aa) 491–506 of TMK39 and 242–254 of TMK54 were synthesised, conjugated to Keyhole Limpet Haemocyanin and used to immunize New Zealand White rabbits. This work was contracted to Covance Research Products Inc., formal animal ethics approval was obtained and animal treatment was in accordance with all applicable laws and regulations. The resultant serum was affinity purified using immobilized peptide and dialysed against PBS. Resulting anti-TMK39 and anti-TMK54 antibodies were stored at −80 °C until use. Antibodies against TMK-96 (PaTMK) and the heavy subunit of the Gal/GalNAc lectin (Hgl) have been previously described (Petri et al., 1989; Boettner et al., 2008). Negative control, anti-Ft, an antibody which is directed against a *Francisella tularensis* protein, was a kind gift from Nicole Ark and Barbara Mann at the University of Virginia, USA. Polyclonal anti-actin (Santa Cruz Biotechnology, Santa Cruz, CA) and monoclonal anti-V5 (Sigma) antibodies were commercially available. For Western blotting, polyclonal antibodies were used at a concentration of 5 μg/ml, whereas monoclonal anti-V5 was used at 1 μg/ml. For confocal microscopy and flow cytometry antibody concentrations were doubled.

2.6. SDS–PAGE gels and Western blotting

Harvested trophozoites (HM-1:IMSS or induced HM-1:IMSS transfectants) were washed in PBS and lysed at a concentration of 10^4 amoebae/μL (50 mM Tris–HCl, pH 8.0, 150 mM NaCl, 1% Nonidet P-40, protease inhibitor cocktail (Sigma, St. Louis, MO, USA) and 0.02 mM E-64 (Sigma, St. Louis, MO, USA)). Cell lysate, immunoprecipitation or fractionated cellular sub-fractions (below) were resolved in 10% SDS–PAGE gels, transferred to polyvinylidene fluoride membrane using standard methods and membranes were blocked with 5% non-fat dry milk in Tris-buffered saline containing 0.1% (v/v) Tween-20 (TTBS) for 1 h at room temperature (RT). If noted, the membrane was cut into strips or primary antibodies (5 μg/ml) were pre-incubated with the indicated amount of unconjugated peptide for 1 h at RT prior to use. Primary antibodies diluted in TTBS were incubated with blocked membranes for 1 h at RT, membranes were washed with TTBS (5 × 5 min) and exposed to secondary antibody (anti-rabbit:AP or anti-mouse:AP) at a concentration recommended by the manufacturer (Sigma, St. Louis, MO, USA) for 1 h at RT. Finally, membranes were washed five times in TTBS and bands were visualised on film using the enhanced chemiluminescent (ECL) kit (Roche, Indianapolis, IN, USA).

2.7. Flow cytometry

Late-log phase *E. histolytica* trophozoites were harvested, washed twice with PBS and fixed with 3.7% paraformaldehyde (PFA) in PBS for 30 min at RT. If indicated, cells were permeabilized for 1 min with 0.2% Triton X-100 (Sigma, St. Louis, MO, USA) in PBS and non-specific binding was blocked by incubation with 20% goat serum and 5% BSA for 1 h at 37 °C. To assess TMK levels, permeabilized HM-1:IMSS trophozoites were stained for 1 h at 37 °C with anti-TMK39, anti-TMK54, anti-PaTMK (TMK-96), anti-Hgl (as a positive control) or anti-Ft (as a negative control).

To assess lectin levels, both non-permeabilized (cell surface Hgl) and permeabilized (total Hgl) transfected trophozoites were stained with anti-Hgl for 1 h at 37 °C. In both instances, Cy™ 3-conjugated Goat Anti-Rabbit IgG (Jackson Immuno Research, West Grove, PA, USA) was used as the secondary antibody at a 1:200 dilution in blocking buffer. As a control, cells were stained with secondary antibody only (no primary antibody). After 1 h incubation at 37 °C with the secondary antibody, samples were washed three times in PBS, re-suspended in 200 μl of PBS and analysed using a FACSCalibur (BD Biosciences) on channel FL2. In all instances, an intact amoeba gate was set prior to data collection (using side scatter (SSC) and forward scatter (FSC) and 10,000 gated events were collected for each sample. FlowJo software (http://www.treestar.com/flowjo/) was used for data analysis. All experiments were carried out three times or more and representative overlaid FL2 histograms are shown.

2.8. Fractionation

Cellular fractionation was carried out as previously described (Aley et al., 1980). Briefly, 10^8 trophozoites were harvested, washed twice with 19 mM potassium phosphate buffer, pH 7.2, and 0.27 M NaCl (PD). Cells were re-suspended to 2×10^7 amoebae/ml in PD + 10 mM $MgCl_2$ and mixed with an equal volume of 1 mg/ml concanavalin A in the same buffer. After 5 min at RT, cells were centrifuged at 50g for 1 min and the supernatant (containing excess conA) was discarded. The pellet was re-suspended in 12 ml of a hypotonic buffer containing 10 mM Tris–HCl, pH 7.5, 2 mM PMSF (Tris buffer) and 1 mM $MgCl_2$. After a 10 min swell, the cells were homogenised using 18–20 strokes of a glass Dounce homogenizer. A two-step gradient consisting of 0.5 M mannitol (8 ml) over 0.58 M sucrose (4 ml), both in Tris buffer, was prepared (gradient 1). The homogenate was layered on top and then centrifuged at 250g for 30 min. Large plasma membrane fragments formed a pellet at the bottom of gradient 1. The material remaining above gradient 1 was spun at 40,000g for 1 h to separate soluble cytoplasmic components (supernatant) from internal membranes (pellet). The plasma membrane pellet from the bottom of gradient 1 was re-suspended in 1 ml of Tris buffer + 1 M α-methyl mannoside and iced for 40 min with occasional mixing. The mixture was diluted into 3 volume of Tris buffer and homogenised with 80 strokes of a Dounce homogenizer. The homogenate was layered onto 20% sucrose in Tris buffer (gradient 2) and centrifuged at 250g for 30 min. Vesiculated plasma membranes that remained above gradient 2 were collected and concentrated by centrifugation at 40,000g for 1 h. The resulting pellet was re-suspended in Tris buffer and served as the plasma membrane fraction.

The three fractions used for analysis (soluble, internal membranes, and plasma membranes) were adjusted to equal volumes and analysed by Western blotting. As TMK39 and Hgl are similar in size (respectively, 127 kDa and 170 kDa), membrane panels

were first probed with anti-TMK antibodies and developed, then stripped with ReBlot Plus Strong Antibody Stripping solution (Millipore, Billerica, MA, USA) and re-probed with anti-Hgl antibodies.

2.9. Confocal microscopy

E. histolytica trophozoites (HM-1:IMSS) in TYI-S-33 medium were allowed to adhere to glass coverslips in a 24-well plate for 1 h at 37 °C at a concentration of 5.0×10^5 trophozoites/well. Adherent amoebae were washed with warm PBS and fixed with 3.7% PFA for 30 min at RT. Non-specific binding was blocked with 20% goat serum and 5% BSA (Sigma, St. Louis, MO, USA) in PBS (1 h at 37 °C). Cells were stained for 1 h at 37 °C with anti-TMK antibodies diluted in blocking buffer. If indicated, primary antibodies were pre-incubated with 300 nM unconjugated peptide for 1 h at RT. Cells were then washed three times with PBS and Cy3-conjugated goat anti-rabbit secondary antibodies (Jackson Laboratories, Bar Harbor, ME, USA) were added at a 1:200 dilution (in blocking buffer) for 1 h at 37 °C. After three washes, coverslips were mounted to slides with Fluoromount-G (Southern BioTech, Birmingham, AL, USA). A Zeiss LSM 510 laser-scanning microscope was used to visualise cells and final images were analysed using LSM Image Browser software (Carl Zeiss, Inc., Thornwood, NY, USA).

2.10. Inducible expression vectors

For expression of truncated proteins containing V5 and 6× His tags, the indicated regions of TMK39 and TMK54 were PCR amplified with the primers: 39F -CACC ATG TTT CTT TTA TTT ACA ATC CTC, 39R -AAT AAT AAT AAG AAT AAT CAC AAT CAG, 54F -CACC ATG TTG CTT CTT TTT TCA CTT ATT TCA, 54R -ACC AAG AAA TAT TAA AAT AGA TAA TAT AG. These fragments were cloned into the Gateway pENTR™/SD/D-TOPO® (Invitrogen) plasmid, sequence verified and Gateway® LR Clonase™ II Enzyme Mix (Invitrogen) was used, according to manufacturer's instructions, to transfer the truncated TMK fragments into the Gateway® pET-DEST42 vector in-frame with the C-terminal epitope tags. Truncated TMK fragments and tags were then PCR amplified from the pET-DEST42 vector with N-terminal *Kpn*I and C-terminal *Bam*HI restriction sites using the primers: K39F -CTA CTG GGT ACC ATG TTT CTT TTA TTT ACA ATC CTC, K54F -CTA CTG GGT ACC ATG TTG CTT CTT TTT TCA CTT ATT TCA, *Bam*HisR -ATA ATG GGA TCC TCA ATG GTG ATG GTG ATG ATG. Resulting PCR products were cloned into the *Kpn*I and *Bam*HI sites of the digested and gel purified pEhHYG-tetR-O-CAT vector (Hamann et al., 1997). Final constructs were sequence verified and the parental pEhHYG-tetR-O-CAT vector was used as a control.

2.11. Transfection of E. histolytica trophozoites

The GenElute™ HP Plasmid Maxiprep Kit (Sigma, St. Louis, MO, USA) was used to prepare plasmid DNA and DNA was quantified using the NanoDrop™ 2000 (Thermo Fisher, Wilmington, DE, USA). A known quantity of DNA was precipitated using standard methods and re-suspended to a concentration of 200 μg/ml in supplemented (5.7 mM cysteine, 25 mM HEPES and 0.6 mM ascorbic acid) and filter-sterilized Medium 199 (M199S) (Invitrogen, Carlsbad, CA, USA), that had been adjusted to pH 7.0. One hundred microlitre of the DNA (20 μg) was mixed with 15 μl of Attractene or SuperFect (Qiagen, Valencia, CA, USA) and incubated as per the manufacturer's instructions to allow formation of transfection complexes. Log-phase trophozoites were then harvested on ice, washed in M199S and re-suspended to a concentration of 5.0×10^5 amoebae/ml in M199S supplemented with 15% heat-inactivated bovine serum. Processed amoebae (0.9 ml) were added to transfection complexes and incubated for 3 h at 37 °C. After the incubation period, amoebae were added to 25 cm^2 tissue culture flasks containing complete TYI-S-33 medium supplemented with 100 U/ml of penicillin and 100 μg/ml streptomycin (Invitrogen, Carlsbad, CA, USA). After 18 h at 37 °C, transfected cells were selected using 15 μg/ml hygromycin (Invitrogen, Carlsbad, CA, USA). Debris from dead cells was removed and fresh media added beginning 4–5 days post-selection. Approximately 2 weeks after selection, transfectants obtained log-phase growth. Following 24 h of induction with 10 μg/ml of tetracycline, expression was verified by Western blotting using a monoclonal anti-V5 antibody (Sigma) as described.

2.12. Immunoprecipitation

Transfected cells were induced for 24 h and lysed on ice at a concentration of 10^7 amoebae/ml in 50 mM Tris–HCl, pH 8.0, 150 mM NaCl, 1% Nonidet P-40, protease inhibitor cocktail (Sigma, St. Louis, MO, USA) and 0.02 mM E-64 (Sigma). Cellular debris was removed by centrifugation at 9500*g* for 10 min at 4 °C. V5-agarose was washed in PBS five times and 20 μl of the washed agarose was added to 100 μl of cleared lysate. The mixture was incubated for 1.5 h at 4 °C on a shaker. Following the incubation period, the resin was washed three times in lysis buffer diluted 1:1 with PBS and twice in PBS. Twenty microlitre PBS and 5 μl 5× SDS–PAGE sample buffer were added to the agarose; the samples were heated to 95 °C for 10 min and analysed via Western blot.

2.13. Growth curves

Transfected (parental vector, t-39 or t-54) and non-transfected HM-1:IMSS trophozoites were harvested during log-phase growth and 10,000 cells were seeded into 15 ml of TYI-S-33 media that contained 10 μg/ml of tetracycline. Parasite numbers were recorded every 24 h for 4 days and expression of the protein was verified each day, in parallel. At least two independently transfected clones were tested, each sample was assayed in triplicate and results represent the mean of three or more experiments.

2.14. Amnis Imagestream data collection and analysis

Phagocytosis assays were carried out as described below, using 2×10^6 *E. histolytica* trophozoites and 2×10^7 carboxylate-modified 2.0 μm fluorescent yellow-green beads (Sigma, St. Louis, MO, USA). Following PFA fixation, amoebae were permeabilized with 0.2% Triton X-100 in PBS for 1 min if indicated and paraformaldehyde was neutralised with 50 mM NH_4Cl. Non-specific binding was then blocked by incubation (1 h at 37 °C) with 10% goat serum in PBS (blocking buffer). TMKs were detected by incubation for 1 h at 37 °C with anti-TMK antibodies diluted to 15 μg/ml in blocking buffer. Three PBS washes were performed and R-PE-conjugated goat anti-rabbit secondary antibodies (Jackson Laboratories, Bar Harbor, ME, USA) were added at a 1:200 dilution for 1 h at 37 °C. Following the incubation, samples were washed with PBS three times, re-suspended in 50 μl PBS and filtered through a 70 μm nylon cell strainer (BD Falcon, Bedford, MA, USA). Where indicated the procedure was carried out in the absence of amoebae (stained beads) or in the absence of anti-TMK antibodies (secondary only). At least 5000 images were collected using the Amnis Imagestream imaging cytometer (Amnis Corporation; Seattle, WA, USA) and ImageStream Data Exploration and Analysis Software (IDEAS) was used for data analysis. Prior to data analysis, spectral compensation was performed using "stained" beads and stained cells. Raw image files from the same experiment were all compensated with the same matrix and all compensated image files from the same experiment were opened with the same template. In each

template, gating was performed to generate a population of single, in-focus, bead-positive cell images (usually yielding 500–1000 images per sample) and masking was used to identify beads and the brightest 20% of antibody staining. Within the template, the Bright Detail Similarity (BDS) feature was used to calculate the extent of correlation between the two masks and thus quantify the extent of co-localisation between ingested beads and TMKs. BDS scores $\geqslant 3$ are considered co-localised.

2.15. Fluorescent labelling and killing of cells

Ficoll-Paque™ Plus (GE Healthcare, UK) isolated Jurkat cells or packed erythrocytes were suspended in 0.1% BSA in PBS at a concentration of 5×10^6/ml and incubated with 5 μM carboxyfluorescein succinimidyl ester (CFSE) for 10 min at 37 °C. FBS was used to quench unbound dye and the cells were washed three times with RPMI media. Jurkat cells were then killed using UV irradiation, whereas erythrocytes were calcium-treated by incubation at 37 °C for 48 h in HEPES buffer containing 2.5 mM $CaCl_2$. Both methods have been described elsewhere (Bratosin et al., 2001; Teixeira and Huston, 2008).

2.16. Phagocytosis assays

Phagocytosis was assayed by flow cytometry as previously described (Huston et al., 2003). Particles used for ingestion assays included fluorescent green 2.0 μm carboxylate-modified latex beads (Sigma, St. Louis, MO, USA), CFSE-labelled apoptotic Jurkat cells and Ca^{2+} treated red blood cells. Amoebae were induced with 10 μg/ml of tetracycline for 24 h. Particles were then mixed with amoebae at a 5:1 ratio, centrifuged for 5 min at 200*g* and incubated at 37 °C for 30 min. D-Galactose (110 mM) in ice-cold PBS was used to wash away non-ingested material and cells were fixed with 3.7% PFA. Samples were washed, re-suspended in PBS and analysed using a FACSCalibur (BD Biosciences) on channel FL1. SSC and FSC were used to distinguish amoebae from non-ingested particles and a live cell gate was established prior to data collection with 10,000 gated events collected for each sample. The mean fluorescence intensity (MFI) was calculated for each sample, background fluorescence was subtracted and data was plotted as a percentage of control MFI. Cell types were assayed in duplicate (at minimum) and the experiments were repeated at least three times. Data represents the mean of all experiments and error bars represent the SD.

2.17. Pinocytosis assay

Pinocytosis was assayed in a similar manner to phagocytosis, however 1 mg/ml FITC-dextran (Sigma) in PBS was incubated with amoebae instead of a particle. Incubation times and procedures were otherwise the same.

3. Results

3.1. Single cell TMK gene expression analysis

LCM was used in conjunction with microarray analysis to examine TMK gene expression at the single cell level. RNA isolated from a laser-captured *E. histolytica* trophozoite was subjected to two cycles of amplification and analysed via microarray (Supplementary Fig. S1). Affymetrix® GCOS was then used to generate detection calls for each TMK probe set. Multiple TMK transcripts were detected as present within a single cell (Table 1). The experiment was carried out in duplicate and TMK transcripts identified within both cells are underlined in Table 1. Average log intensity values for TMKs and reference genes are listed in Supplementary Table S2. Multiple TMK genes were expressed in both cells, and one cell expressed detectable levels of multiple members of TMK sub-groups A, B_1, D_1 and E. Microarray results were validated by qRT-PCR conducted on RNA isolated from an independently laser-captured trophozoite (data not shown). The presence of multiple TMK transcripts within a single cell indicated that these genes do not undergo antigenic variation at the level of transcription.

3.2. Protein expression analysis

To enable examination of TMK expression at the protein level, polyclonal antibodies directed against unique peptides within the extracellular domains of TMK39 (sub-family C) and TMK54 (sub-family E) were generated. Peptides were chosen for immunization by first manually identifying hydrophilic and cysteine-free stretches of sequence in each extracellular domain and then using the Basic Local Alignment Search Tool (BLAST) to check the sequences against the *E. histolytica* Genome Project Database and ensure specificity. Resultant antibodies were deemed specific as both recognised single bands of the predicted size in *E. histolytica* lysate and both bands disappeared when the antibodies were pre-incubated with increasing amounts of the corresponding unconjugated peptide (Fig. 1A). An anti-peptide antibody against PaTMK (TMK-96, sub-family B_3) has previously been developed and was also used in the following studies (Boettner et al., 2008).

Expression of PaTMK and sub-family B_1 TMKs has been examined at the protein level (Mehra et al., 2006; Boettner et al., 2008) however studies have been limited to Western blotting and microscopy. Consequently, it is unknown whether TMKs are heterogeneously expressed by trophozoites within a population. To examine expression of TMKs at the population level, we labelled permeabilized trophozoites with anti-TMK39, anti-TMK54 or anti-PaTMK, and analysed the samples by flow cytometry. In these experiments, trophozoites were harvested from the same flask, immediately fixed with 3.7% PFA and then stained. Flow cytometric

Table 1
Transmembrane kinase (TMK) transcripts detected in a single, *Entamoeba histolytica* trophozoite. Single cells expressed more than one TMK. RNA from a single amoeba isolated by laser-capture microdissection (LCM) was purified using the PicoPure™ RNA Isolation Kit and subjected to two cycles of amplification using the WT-Ovation™ Pico System. Resulting cDNA was hybridized to the E_his-1a520285 custom array (Affymetrix). The arrays were then stained using the standard Affymetrix protocol for eukaryotic targets. An Affymetrix Gene Chip scanner 3000 I was used to scan the arrays and report files were generated to determine the percentage of present calls. The experiment was carried out twice. TMK transcripts identified are listed, with those identified in both amoebae underlined. Validation of microarray results was carried out by quantitative reverse transcription PCR (qRT-PCR) (data not shown). cDNA samples used for microarray analysis and qRT-PCR validation were generated from different amoebae. For the validation, RNA was purified from a single cell and amplified (two rounds) as described. The mRNA abundance of two GCOS "present" (XM648585 and XM648643) and two GCOS "absent" (XM643895 and XM650501) transcripts was then measured by qRT-PCR. There was agreement in every instance.

TMK group	TMK#	GenBank XM#
A	TMK17	XM646584
	TMK23	XM647001
	TMK65	XM649022
B_1	TMK14	XM646638
	TMK87	XM644636
B_3	TMK35	XM645723
D_1	TMK03	XM646909
	TMK40	XM648928
D_2	TMK19	XM646939
E	TMK22	XM651330
	TMK54	XM648585
F	TMK06	XM644657
	TMK59	XM644333